

[Section 3.3](#) explains how shaders function. For now, what you need to know is that a shader core is a small processor that does some relatively isolated task, such as transforming a vertex from its location in the world to a screen coordinate, or computing the color of a pixel covered by a triangle. With thousands or millions of triangles being sent to the screen each frame, every second there can be billions of *shader invocations*, that is, separate instances where shader programs are run.

To begin with, *latency* is a concern that all processors face. Accessing data takes some amount of time. A basic way to think about latency is that the farther away the information is from the processor, the longer the wait. [Section 23.3](#) covers latency in more detail. Information stored in memory chips will take longer to access than that in local registers. [Section 18.4.1](#) discusses memory access in more depth. The key point is that waiting for data to be retrieved means the processor is stalled, which reduces performance.

3.1 Data-Parallel Architectures

Various strategies are used by different processor architectures to avoid stalls. A CPU is optimized to handle a wide variety of data structures and large code bases. CPUs can have multiple processors, but each runs code in a mostly serial fashion, limited SIMD vector processing being the minor exception. To minimize the effect of latency, much of a CPU's chip consists of fast local caches, memory that is filled with data likely to be needed next. CPUs also avoid stalls by using clever techniques such as branch prediction, instruction reordering, register renaming, and cache prefetching [715].

GPUs take a different approach. Much of a GPU's chip area is dedicated to a large set of processors, called *shader cores*, often numbering in the thousands. The GPU is a stream processor, in which ordered sets of similar data are processed in turn. Because of this similarity—a set of vertices or pixels, for example—the GPU can process these data in a massively parallel fashion. One other important element is that these invocations are as independent as possible, such that they have no need for information from neighboring invocations and do not share writable memory locations. This rule is sometimes broken to allow new and useful functionality, but such exceptions come at a price of potential delays, as one processor may wait on another processor to finish its work.

The GPU is optimized for *throughput*, defined as the maximum rate at which data can be processed. However, this rapid processing has a cost. With less chip area dedicated to cache memory and control logic, latency for each shader core is generally considerably higher than what a CPU processor encounters [462].

Say a mesh is rasterized and two thousand pixels have fragments to be processed; a pixel shader program is to be invoked two thousand times. Imagine there is only a single shader processor, the world's weakest GPU. It starts to execute the shader program for the first fragment of the two thousand. The shader processor performs a few arithmetic operations on values in registers. Registers are local and quick to

access, so no stall occurs. The shader processor then comes to an instruction such as a texture access; e.g., for a given surface location the program needs to know the pixel color of the image applied to the mesh. A texture is an entirely separate resource, not a part of the pixel program's local memory, and texture access can be somewhat involved. A memory fetch can take hundreds to thousands of clock cycles, during which time the GPU processor is doing nothing. At this point the shader processor would stall, waiting for the texture's color value to be returned.

To make this terrible GPU into something considerably better, give each fragment a little storage space for its local registers. Now, instead of stalling on a texture fetch, the shader processor is allowed to switch and execute another fragment, number two of two thousand. This switch is extremely fast, nothing in the first or second fragment is affected other than noting which instruction was executing on the first. Now the second fragment is executed. Same as with the first, a few arithmetic functions are performed, then a texture fetch is again encountered. The shader core now switches to another fragment, number three. Eventually all two thousand fragments are processed in this way. At this point the shader processor returns to fragment number one. By this time the texture color has been fetched and is available for use, so the shader program can then continue executing. The processor proceeds in the same fashion until another instruction that is known to stall execution is encountered, or the program completes. A single fragment will take longer to execute than if the shader processor stayed focused on it, but overall execution time for the fragments as a whole is dramatically reduced.

In this architecture, latency is hidden by having the GPU stay busy by switching to another fragment. GPUs take this design a step further by separating the instruction execution logic from the data. Called *single instruction, multiple data* (SIMD), this arrangement executes the same command in lock-step on a fixed number of shader programs. The advantage of SIMD is that considerably less silicon (and power) needs to be dedicated to processing data and switching, compared to using an individual logic and dispatch unit to run each program. Translating our two-thousand-fragment example into modern GPU terms, each pixel shader invocation for a fragment is called a *thread*. This type of thread is unlike a CPU thread. It consists of a bit of memory for the input values to the shader, along with any register space needed for the shader's execution. Threads that use the same shader program are bundled into groups, called *warps* by NVIDIA and *wavefronts* by AMD. A warp/wavefront is scheduled for execution by some number GPU shader cores, anywhere from 8 to 64, using SIMD-processing. Each thread is mapped to a *SIMD lane*.

Say we have two thousand threads to be executed. Warps on NVIDIA GPUs contain 32 threads. This yields $2000/32 = 62.5$ warps, which means that 63 warps are allocated, one warp being half empty. A warp's execution is similar to our single GPU processor example. The shader program is executed in lock-step on all 32 processors. When a memory fetch is encountered, all threads encounter it at the same time, because the same instruction is executed for all. The fetch signals that this warp of threads will stall, all waiting for their (different) results. Instead of stalling, the

warp is swapped out for a different warp of 32 threads, which is then executed by the 32 cores. This swapping is just as fast as with our single processor system, as no data within each thread is touched when a warp is swapped in or out. Each thread has its own registers, and each warp keeps track of which instruction it is executing. Swapping in a new warp is just a matter of pointing the set of cores at a different set of threads to execute; there is no other overhead. Warps execute or swap out until all are completed. See [Figure 3.1](#).

In our simple example the latency of a memory fetch for a texture can cause a warp to swap out. In reality warps could be swapped out for shorter delays, since the cost of swapping is so low. There are several other techniques used to optimize execution [945], but warp-swapping is the major latency-hiding mechanism used by all GPUs. Several factors are involved in how efficiently this process works. For example, if there are few threads, then few warps can be created, making latency hiding problematic.

The shader program's structure is an important characteristic that influences efficiency. A major factor is the amount of register use for each thread. In our example we assume that two thousand threads can all be resident on the GPU at one time. The more registers needed by the shader program associated with each thread, the fewer threads, and thus the fewer warps, can be resident in the GPU. A shortage of warps can mean that a stall cannot be mitigated by swapping. Warps that are resident are said to be “in flight,” and this number is called the *occupancy*. High occupancy means that there are many warps available for processing, so that idle processors are less likely. Low occupancy will often lead to poor performance. The frequency of memory fetches also affects how much latency hiding is needed. Lauritzen [993] outlines how occupancy is affected by the number of registers and the shared memory that a shader uses. Wronski [1911, 1914] discusses how the ideal occupancy rate can vary depending on the type of operations a shader performs.

Another factor affecting overall efficiency is dynamic branching, caused by “if” statements and loops. Say an “if” statement is encountered in a shader program. If all the threads evaluate and take the same branch, the warp can continue without any concern about the other branch. However, if some threads, or even one thread, take the alternate path, then the warp must execute both branches, throwing away the results not needed by each particular thread [530, 945]. This problem is called *thread divergence*, where a few threads may need to execute a loop iteration or perform an “if” path that the other threads in the warp do not, leaving them idle during this time.

All GPUs implement these architectural ideas, resulting in systems with strict limitations but massive amounts of compute power per watt. Understanding how this system operates will help you as a programmer make more efficient use of the power it provides. In the sections that follow we discuss how the GPU implements the rendering pipeline, how programmable shaders operate, and the evolution and function of each GPU stage.

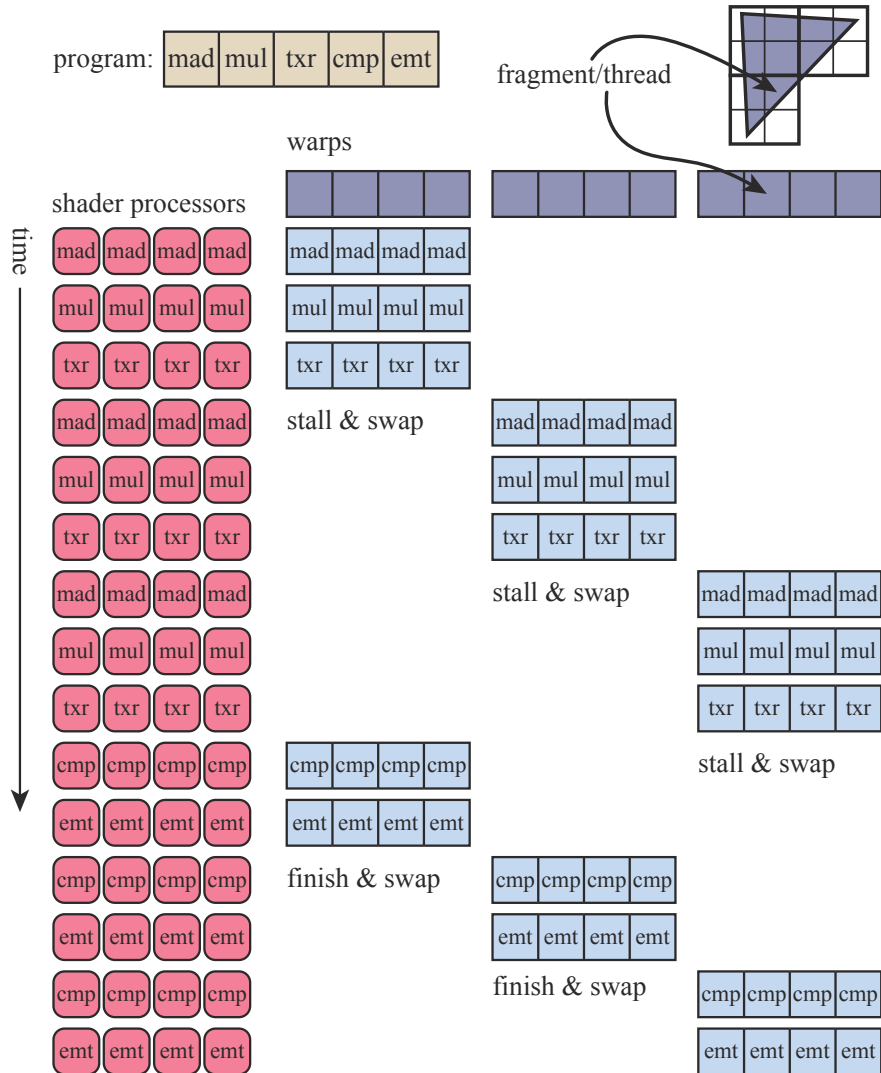


Figure 3.1. Simplified shader execution example. A triangle's fragments, called threads, are gathered into warps. Each warp is shown as four threads but have 32 threads in reality. The shader program to be executed is five instructions long. The set of four GPU shader processors executes these instructions for the first warp until a stall condition is detected on the “txr” command, which needs time to fetch its data. The second warp is swapped in and the shader program’s first three instructions are applied to it, until a stall is again detected. After the third warp is swapped in and stalls, execution continues by swapping in the first warp and continuing execution. If its “txr” command’s data are not yet returned at this point, execution truly stalls until these data are available. Each warp finishes in turn.

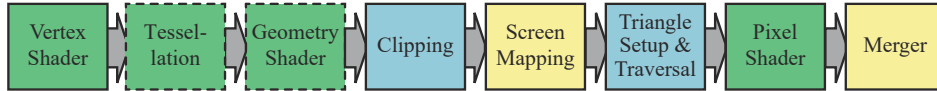


Figure 3.2. GPU implementation of the rendering pipeline. The stages are color coded according to the degree of user control over their operation. Green stages are fully programmable. Dashed lines show optional stages. Yellow stages are configurable but not programmable, e.g., various blend modes can be set for the merge stage. Blue stages are completely fixed in their function.

3.2 GPU Pipeline Overview

The GPU implements the conceptual geometry processing, rasterization, and pixel processing pipeline stages described in [Chapter 2](#). These are divided into several hardware stages with varying degrees of configurability or programmability. [Figure 3.2](#) shows the various stages color coded according to how programmable or configurable they are. Note that these physical stages are split up somewhat differently than the functional stages presented in [Chapter 2](#).

We describe here the *logical model* of the GPU, the one that is exposed to you as a programmer by an API. As [Chapters 18](#) and [23](#) discuss, the implementation of this logical pipeline, the *physical model*, is up to the hardware vendor. A stage that is fixed-function in the logical model may be executed on the GPU by adding commands to an adjacent programmable stage. A single program in the pipeline may be split into elements executed by separate sub-units, or be executed by a separate pass entirely. The logical model can help you reason about what affects performance, but it should not be mistaken for the way the GPU actually implements the pipeline.

The vertex shader is a fully programmable stage that is used to implement the geometry processing stage. The geometry shader is a fully programmable stage that operates on the vertices of a primitive (point, line, or triangle). It can be used to perform per-primitive shading operations, to destroy primitives, or to create new ones. The tessellation stage and geometry shader are both optional, and not all GPUs support them, especially on mobile devices.

The clipping, triangle setup, and triangle traversal stages are implemented by fixed-function hardware. Screen mapping is affected by window and viewport settings, internally forming a simple scale and repositioning. The pixel shader stage is fully programmable. Although the merger stage is not programmable, it is highly configurable and can be set to perform a wide variety of operations. It implements the “merging” functional stage, in charge of modifying the color, z-buffer, blend, stencil, and any other output-related buffers. The pixel shader execution together with the merger stage form the conceptual pixel processing stage presented in [Chapter 2](#).

Over time, the GPU pipeline has evolved away from hard-coded operation and toward increasing flexibility and control. The introduction of programmable shader stages was the most important step in this evolution. The next section describes the features common to the various programmable stages.

3.3 The Programmable Shader Stage

Modern shader programs use a unified shader design. This means that the vertex, pixel, geometry, and tessellation-related shaders share a common programming model. Internally they have the same *instruction set architecture* (ISA). A processor that implements this model is called a *common-shader core* in DirectX, and a GPU with such cores is said to have a unified shader architecture. The idea behind this type of architecture is that shader processors are usable in a variety of roles, and the GPU can allocate these as it sees fit. For example, a set of meshes with tiny triangles will need more vertex shader processing than large squares each made of two triangles. A GPU with separate pools of vertex and pixel shader cores means that the ideal work distribution to keep all the cores busy is rigidly predetermined. With unified shader cores, the GPU can decide how to balance this load.

Describing the entire shader programming model is well beyond the scope of this book, and there are many documents, books, and websites that already do so. Shaders are programmed using C-like *shading languages* such as DirectX’s *High-Level Shading Language* (HLSL) and the *OpenGL Shading Language* (GLSL). DirectX’s HLSL can be compiled to virtual machine bytecode, also called the *intermediate language* (IL or DXIL), to provide hardware independence. An intermediate representation can also allow shader programs to be compiled and stored offline. This intermediate language is converted to the ISA of the specific GPU by the driver. Console programming usually avoids the intermediate language step, since there is then only one ISA for the system.

The basic data types are 32-bit single-precision floating point scalars and vectors, though vectors are only part of the shader code and are not supported in hardware as outlined above. On modern GPUs 32-bit integers and 64-bit floats are also supported natively. Floating point vectors typically contain data such as positions ($xyzw$), normals, matrix rows, colors ($rgba$), or texture coordinates ($uvwq$). Integers are most often used to represent counters, indices, or bitmasks. Aggregate data types such as structures, arrays, and matrices are also supported.

A *draw call* invokes the graphics API to draw a group of primitives, so causing the graphics pipeline to execute and run its shaders. Each programmable shader stage has two types of inputs: *uniform* inputs, with values that remain constant throughout a draw call (but can be changed between draw calls), and *varying* inputs, data that come from the triangle’s vertices or from rasterization. For example, a pixel shader may provide the color of a light source as a uniform value, and the triangle surface’s location changes per pixel and so is varying. A texture is a special kind of uniform input that once was always a color image applied to a surface, but that now can be thought of as any large array of data.

The underlying virtual machine provides special registers for the different types of inputs and outputs. The number of available *constant registers* for uniforms is much larger than those registers available for varying inputs or outputs. This happens because the varying inputs and outputs need to be stored separately for each vertex

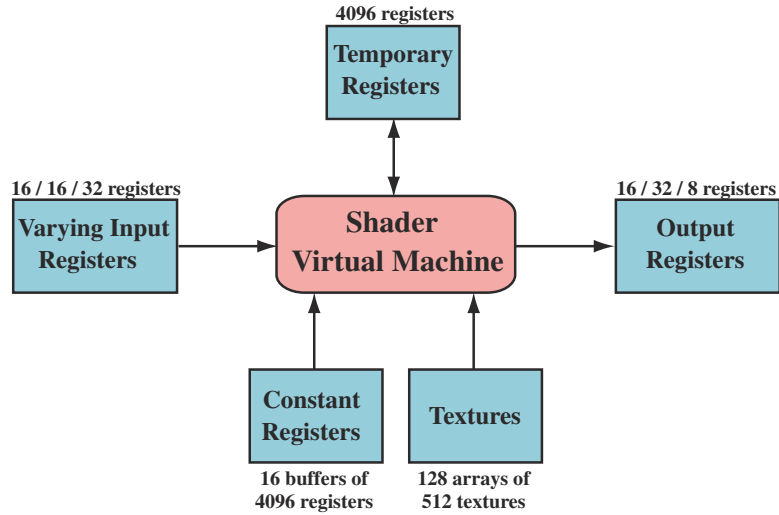


Figure 3.3. Unified virtual machine architecture and register layout, under Shader Model 4.0. The maximum available number is indicated next to each resource. Three numbers separated by slashes refer to the limits for vertex, geometry, and pixel shaders (from left to right).

or pixel, so there is a natural limit as to how many are needed. The uniform inputs are stored once and reused across all the vertices or pixels in the draw call. The virtual machine also has general-purpose *temporary registers*, which are used for scratch space. All types of registers can be array-indexed using integer values in temporary registers. The inputs and outputs of the shader virtual machine can be seen in Figure 3.3.

Operations that are common in graphics computations are efficiently executed on modern GPUs. Shading languages expose the most common of these operations (such as additions and multiplications) via operators such as `*` and `+`. The rest are exposed through *intrinsic functions*, e.g., `atan()`, `sqrt()`, `log()`, and many others, optimized for the GPU. Functions also exist for more complex operations, such as vector normalization and reflection, the cross product, and matrix transpose and determinant computations.

The term *flow control* refers to the use of branching instructions to change the flow of code execution. Instructions related to flow control are used to implement high-level language constructs such as “if” and “case” statements, as well as various types of loops. Shaders support two types of flow control. *Static flow control* branches are based on the values of uniform inputs. This means that the flow of the code is constant over the draw call. The primary benefit of static flow control is to allow the same shader to be used in a variety of different situations (e.g., a varying number of lights). There is no thread divergence, since all invocations take the same code path. *Dynamic flow control* is based on the values of varying inputs, meaning that each

fragment can execute the code differently. This is much more powerful than static flow control but can cost performance, especially if the code flow changes erratically between shader invocations.

3.4 The Evolution of Programmable Shading and APIs

The idea of a framework for programmable shading dates back to 1984 with Cook's *shade trees* [287]. A simple shader and its corresponding shade tree are shown in Figure 3.4. The RenderMan Shading Language [63, 1804] was developed from this idea in the late 1980s. It is still used today for film production rendering, along with other evolving specifications, such as the *Open Shading Language* (OSL) project [608].

Consumer-level graphics hardware was first successfully introduced by 3dfx Interactive on October 1, 1996. See Figure 3.5 for a timeline from this year. Their Voodoo graphics card's ability to render the game *Quake* with high quality and performance led to its quick adoption. This hardware implemented a fixed-function pipeline throughout. Before GPUs supported programmable shaders natively, there were several attempts to implement programmable shading operations in real time via multiple rendering passes. The *Quake III: Arena* scripting language was the first widespread

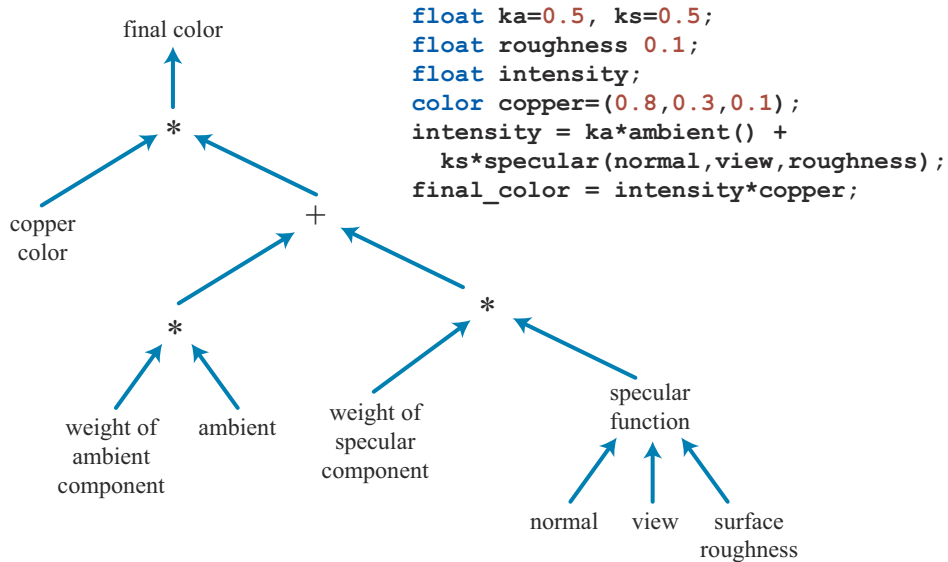


Figure 3.4. Shade tree for a simple copper shader, and its corresponding shader language program. (After Cook [287].)

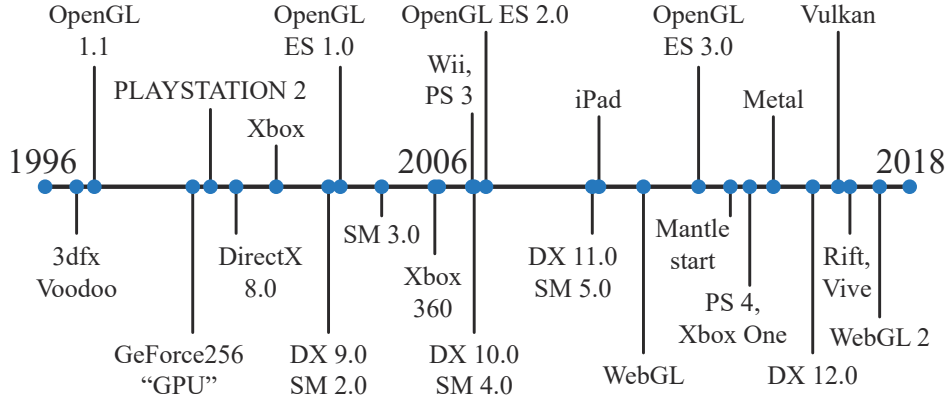


Figure 3.5. A timeline of some API and graphics hardware releases.

commercial success in this area in 1999. As mentioned at the beginning of the chapter, NVIDIA’s GeForce256 was the first hardware to be called a GPU, but it was not programmable. However, it was configurable.

In early 2001, NVIDIA’s GeForce 3 was the first GPU to support programmable vertex shaders [1049], exposed through DirectX 8.0 and extensions to OpenGL. These shaders were programmed in an assembly-like language that was converted by the drivers into microcode on the fly. Pixel shaders were also included in DirectX 8.0, but pixel shaders fell short of actual programmability—the limited “programs” supported were converted into texture blending states by the driver, which in turn wired together hardware “register combiners.” These “programs” were not only limited in length (12 instructions or less) but also lacked important functionality. Dependent texture reads and floating point data were identified by Peercy et al. [1363] as crucial to true programmability, from their study of RenderMan.

Shaders at this time did not allow for flow control (branching), so conditionals had to be emulated by computing both terms and selecting or interpolating between the results. DirectX defined the concept of a *Shader Model* (SM) to distinguish hardware with different shader capabilities. The year 2002 saw the release of DirectX 9.0 including Shader Model 2.0, which featured truly programmable vertex and pixel shaders. Similar functionality was also exposed under OpenGL using various extensions. Support for arbitrary dependent texture reads and storage of 16-bit floating point values was added, finally completing the set of requirements identified by Peercy et al. Limits on shader resources such as instructions, textures, and registers were increased, so shaders became capable of more complex effects. Support for flow control was also added. The growing length and complexity of shaders made the assembly programming model increasingly cumbersome. Fortunately, DirectX 9.0

also included HLSL. This shading language was developed by Microsoft in collaboration with NVIDIA. Around the same time, the OpenGL ARB (Architecture Review Board) released GLSL, a fairly similar language for OpenGL [885]. These languages were heavily influenced by the syntax and design philosophy of the C programming language and included elements from the RenderMan Shading Language.

Shader Model 3.0 was introduced in 2004 and added dynamic flow control, making shaders considerably more powerful. It also turned optional features into requirements, further increased resource limits and added limited support for texture reads in vertex shaders. When a new generation of game consoles was introduced in late 2005 (Microsoft's Xbox 360) and late 2006 (Sony Computer Entertainment's PLAYSTATION 3 system), they were equipped with Shader Model 3.0-level GPUs. Nintendo's Wii console was one of the last notable fixed-function GPUs, which initially shipped in late 2006. The purely fixed-function pipeline is long gone at this point. Shader languages have evolved to a point where a variety of tools are used to create and manage them. A screenshot of one such tool, using Cook's shade tree concept, is shown in Figure 3.6.

The next large step in programmability also came near the end of 2006. Shader Model 4.0, included in DirectX 10.0 [175], introduced several major features, such as the geometry shader and stream output. Shader Model 4.0 included a uniform

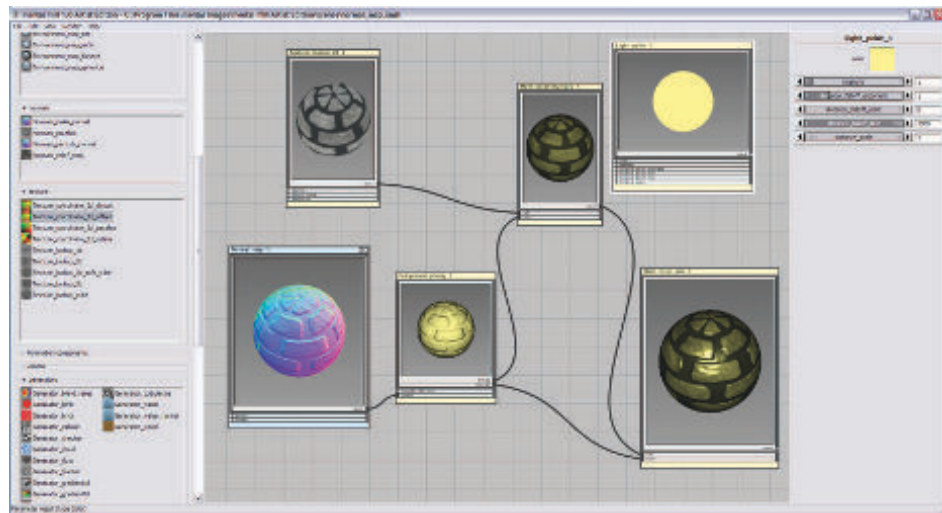


Figure 3.6. A visual shader graph system for shader design. Various operations are encapsulated in function boxes, selectable on the left. When selected, each function box has adjustable parameters, shown on the right. Inputs and outputs for each function box are linked to each other to form the final result, shown in the lower right of the center frame. (*Screenshot from “mental mill,” mental images inc.*)

programming model for all shaders (vertex, pixel, and geometry), the unified shader design described earlier. Resource limits were further increased, and support for integer data types (including bitwise operations) was added. The introduction of GLSL 3.30 in OpenGL 3.3 provided a similar shader model.

In 2009 DirectX 11 and Shader Model 5.0 were released, adding the tessellation stage shaders and the compute shader, also called DirectCompute. The release also focused on supporting CPU multiprocessing more effectively, a topic discussed in [Section 18.5](#). OpenGL added tessellation in version 4.0 and compute shaders in 4.3. DirectX and OpenGL evolve differently. Both set a certain level of hardware support needed for a particular version release. Microsoft controls the DirectX API and so works directly with independent hardware vendors (IHVs) such as AMD, NVIDIA, and Intel, as well as game developers and computer-aided design software firms, to determine what features to expose. OpenGL is developed by a consortium of hardware and software vendors, managed by the nonprofit Khronos Group. Because of the number of companies involved, the API features often appear in a release of OpenGL some time after their introduction in DirectX. However, OpenGL allows *extensions*, vendor-specific or more general, that allow the latest GPU functions to be used before official support in a release.

The next significant change in APIs was led by AMD's introduction of the Mantle API in 2013. Developed in partnership with video game developer DICE, the idea of Mantle was to strip out much of the graphics driver's overhead and give this control directly to the developer. Alongside this refactoring was further support for effective CPU multiprocessing. This new class of APIs focuses on vastly reducing the time the CPU spends in the driver, along with more efficient CPU multiprocessor support ([Chapter 18](#)). The ideas pioneered in Mantle were picked up by Microsoft and released as DirectX 12 in 2015. Note that DirectX 12 is not focused on exposing new GPU functionality—DirectX 11.3 exposed the same hardware features. Both APIs can be used to send graphics to virtual reality systems such as the Oculus Rift and HTC Vive. However, DirectX 12 is a radical redesign of the API, one that better maps to modern GPU architectures. Low-overhead drivers are useful for applications where the CPU driver cost is causing a bottleneck, or where using more CPU processors for graphics could benefit performance [946]. Porting from earlier APIs can be difficult, and a naive implementation can result in lower performance [249, 699, 1438].

Apple released its own low-overhead API called Metal in 2014. Metal was first available on mobile devices such as the iPhone 5S and iPad Air, with newer Macintoshes given access a year later through OS X El Capitan. Beyond efficiency, reducing CPU usage saves power, an important factor on mobile devices. This API has its own shading language, meant for both graphics and GPU compute programs.

AMD donated its Mantle work to the Khronos Group, which released its own new API in early 2016, called Vulkan. As with OpenGL, Vulkan works on multiple operating systems. Vulkan uses a new high-level intermediate language called SPIR-V, which is used for both shader representation and for general GPU computing. Precompiled shaders are portable and so can be used on any GPU supporting the

capabilities needed [885]. Vulkan can also be used for non-graphical GPU computation, as it does not need a display window [946]. One notable difference of Vulkan from other low-overhead drivers is that it is meant to work with a wide range of systems, from workstations to mobile devices.

On mobile devices the norm has been to use OpenGL ES. “ES” stands for Embedded Systems, as this API was developed with mobile devices in mind. Standard OpenGL at the time was rather bulky and slow in some of its call structures, as well as requiring support for rarely used functionality. Released in 2003, OpenGL ES 1.0 was a stripped-down version of OpenGL 1.3, describing a fixed-function pipeline. While releases of DirectX are timed with those of graphics hardware that support them, developing graphics support for mobile devices did not proceed in the same fashion. For example, the first iPad, released in 2010, implemented OpenGL ES 1.1. In 2007 the OpenGL ES 2.0 specification was released, providing programmable shading. It was based on OpenGL 2.0, but without the fixed-function component, and so was not backward-compatible with OpenGL ES 1.1. OpenGL ES 3.0 was released in 2012, providing functionality such as multiple render targets, texture compression, transform feedback, instancing, and a much wider range of texture formats and modes, as well as shader language improvements. OpenGL ES 3.1 adds compute shaders, and 3.2 adds geometry and tessellation shaders, among other features. Chapter 23 discusses mobile device architectures in more detail.

An offshoot of OpenGL ES is the browser-based API WebGL, called through JavaScript. Released in 2011, the first version of this API is usable on most mobile devices, as it is equivalent to OpenGL ES 2.0 in functionality. As with OpenGL, extensions give access to more advanced GPU features. WebGL 2 assumes OpenGL ES 3.0 support.

WebGL is particularly well suited for experimenting with features or use in the classroom:

- It is cross-platform, working on all personal computers and almost all mobile devices.
- Driver approval is handled by the browsers. Even if one browser does not support a particular GPU or extension, often another browser does.
- Code is interpreted, not compiled, and only a text editor is needed for development.
- A debugger is built in to most browsers, and code running at any website can be examined.
- Programs can be deployed by uploading them to a website or Github, for example.

Higher-level scene-graph and effects libraries such as three.js [218] give easy access to code for a variety of more involved effects such as shadow algorithms, post-processing effects, physically based shading, and deferred rendering.

3.5 The Vertex Shader

The vertex shader is the first stage in the functional pipeline shown in [Figure 3.2](#). While this is the first stage directly under programmer control, it is worth noting that some data manipulation happens before this stage. In what DirectX calls the *input assembler* [175, 530, 1208], several streams of data can be woven together to form the sets of vertices and primitives sent down the pipeline. For example, an object could be represented by one array of positions and one array of colors. The input assembler would create this object’s triangles (or lines or points) by creating vertices with positions and colors. A second object could use the same array of positions (along with a different model transform matrix) and a different array of colors for its representation. Data representation is discussed in detail in [Section 16.4.5](#). There is also support in the input assembler to perform *instancing*. This allows an object to be drawn several times with some varying data per instance, all with a single draw call. The use of instancing is covered in [Section 18.4.2](#).

A triangle mesh is represented by a set of vertices, each associated with a specific position on the model surface. Besides position, there are other optional properties associated with each vertex, such as a color or texture coordinates. Surface normals are defined at mesh vertices as well, which may seem like an odd choice. Mathematically, each triangle has a well-defined surface normal, and it may seem to make more sense to use the triangle’s normal directly for shading. However, when rendering, triangle meshes are often used to represent an underlying curved surface, and vertex normals are used to represent the orientation of this surface, rather than that of the triangle mesh itself. [Section 16.3.4](#) will discuss methods to compute vertex normals. [Figure 3.7](#) shows side views of two triangle meshes that represent curved surfaces, one smooth and one with a sharp crease.

The vertex shader is the first stage to process the triangle mesh. The data describing what triangles are formed is unavailable to the vertex shader. As its name implies, it deals exclusively with the incoming vertices. The vertex shader provides a way

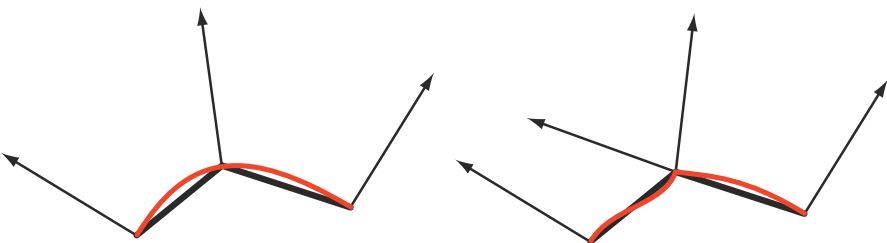


Figure 3.7. Side views of triangle meshes (in black, with vertex normals) representing curved surfaces (in red). On the left smoothed vertex normals are used to represent a smooth surface. On the right the middle vertex has been duplicated and given two normals, representing a crease.

to modify, create, or ignore values associated with each triangle's vertex, such as its color, normal, texture coordinates, and position. Normally the vertex shader program transforms vertices from model space to homogeneous clip space ([Section 4.7](#)). At a minimum, a vertex shader must always output this location.

A vertex shader is much the same as the unified shader described earlier. Every vertex passed in is processed by the vertex shader program, which then outputs a number of values that are interpolated across a triangle or line. The vertex shader can neither create nor destroy vertices, and results generated by one vertex cannot be passed on to another vertex. Since each vertex is treated independently, any number of shader processors on the GPU can be applied in parallel to the incoming stream of vertices.

Input assembly is usually presented as a process that happens before the vertex shader is executed. This is an example where the physical model often differs from the logical. Physically, the fetching of data to create a vertex might happen in the vertex shader and the driver will quietly prepend every shader with the appropriate instructions, invisible to the programmer.

Chapters that follow explain several vertex shader effects, such as vertex blending for animating joints, and silhouette rendering. Other uses for the vertex shader include:

- Object generation, by creating a mesh only once and having it be deformed by the vertex shader.
- Animating character's bodies and faces using skinning and morphing techniques.
- Procedural deformations, such as the movement of flags, cloth, or water [802, 943].
- Particle creation, by sending degenerate (no area) meshes down the pipeline and having these be given an area as needed.
- Lens distortion, heat haze, water ripples, page curls, and other effects, by using the entire framebuffer's contents as a texture on a screen-aligned mesh undergoing procedural deformation.
- Applying terrain height fields by using vertex texture fetch [40, 1227].

Some deformations done using a vertex shader are shown in [Figure 3.8](#).

The output of the vertex shader can be consumed in several different ways. The usual path is for each instance's primitives, e.g., triangles, to then be generated and rasterized, and the individual pixel fragments produced to be sent to the pixel shader program for continued processing. On some GPUs the data can also be sent to the tessellation stage or the geometry shader or be stored in memory. These optional stages are discussed in the following sections.



Figure 3.8. On the left, a normal teapot. A simple shear operation performed by a vertex shader program produces the middle image. On the right, a noise function creates a field that distorts the model. (*Images produced by FX Composer 2, courtesy of NVIDIA Corporation.*)

3.6 The Tessellation Stage

The tessellation stage allows us to render curved surfaces. The GPU’s task is to take each surface description and turn it into a representative set of triangles. This stage is an optional GPU feature that first became available in (and is required by) DirectX 11. It is also supported in OpenGL 4.0 and OpenGL ES 3.2.

There are several advantages to using the tessellation stage. The curved surface description is often more compact than providing the corresponding triangles themselves. Beyond memory savings, this feature can keep the bus between CPU and GPU from becoming the bottleneck for an animated character or object whose shape is changing each frame. The surfaces can be rendered efficiently by having an appropriate number of triangles generated for the given view. For example, if a ball is far from the camera, only a few triangles are needed. Up close, it may look best represented with thousands of triangles. This ability to control the *level of detail* can also allow an application to control its performance, e.g., using a lower-quality mesh on weaker GPUs in order to maintain frame rate. Models normally represented by flat surfaces can be converted to fine meshes of triangles and then warped as desired [1493], or they can be tessellated in order to perform expensive shading computations less frequently [225].

The tessellation stage always consists of three elements. Using DirectX’s terminology, these are the *hull shader*, *tessellator*, and *domain shader*. In OpenGL the hull shader is the *tessellation control shader* and the domain shader the *tessellation evaluation shader*, which are a bit more descriptive, though verbose. The fixed-function tessellator is called the *primitive generator* in OpenGL, and as will be seen, that is indeed what it does.

How to specify and tessellate curves and surfaces is discussed at length in [Chapter 17](#). Here we give a brief summary of each tessellation stage’s purpose. To begin, the input to the hull shader is a special *patch* primitive. This consists of several control points defining a subdivision surface, Bézier patch, or other type of curved element. The hull shader has two functions. First, it tells the tessellator how many triangles should be generated, and in what configuration. Second, it performs processing on each of the control points. Also, optionally, the hull shader can modify the incoming

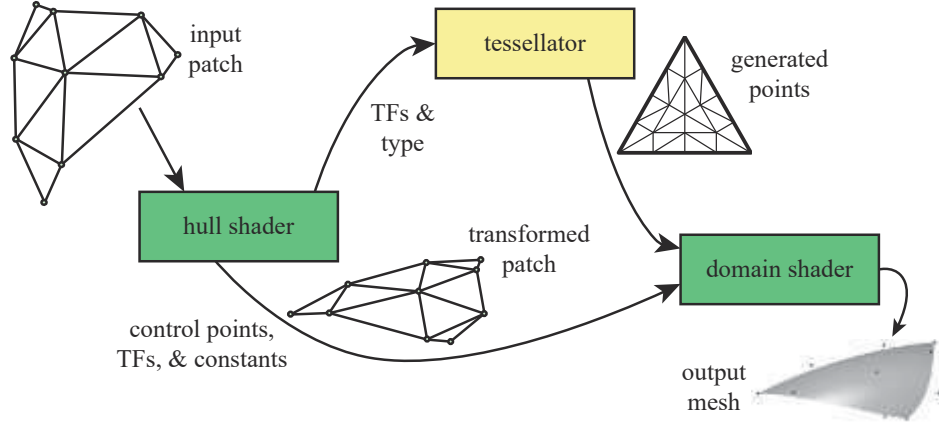


Figure 3.9. The tessellation stage. The hull shader takes in a patch defined by control points. It sends the tessellation factors (TFs) and type to the fixed-function tessellator. The control point set is transformed as desired by the hull shader and sent on to the domain shader, along with TFs and related patch constants. The tessellator creates the set of vertices along with their barycentric coordinates. These are then processed by the domain shader, producing the triangle mesh (control points shown for reference).

patch description, adding or removing control points as desired. The hull shader outputs its set of control points, along with the tessellation control data, to the domain shader. See [Figure 3.9](#).

The tessellator is a fixed-function stage in the pipeline, only used with tessellation shaders. It has the task of adding several new vertices for the domain shader to process. The hull shader sends the tessellator information about what type of tessellation surface is desired: triangle, quadrilateral, or isoline. Isolines are sets of line strips, sometimes used for hair rendering [1954]. The other important values sent by the hull shader are the tessellation factors (*tessellation levels* in OpenGL). These are of two types: inner and outer edge. The two inner factors determine how much tessellation occurs inside the triangle or quadrilateral. The outer factors determine how much each exterior edge is split ([Section 17.6](#)). An example of increasing tessellation factors is shown in [Figure 3.10](#). By allowing separate controls, we can have adjacent curved surfaces' edges match in tessellation, regardless of how the interiors are tessellated. Matching edges avoids cracks or other shading artifacts where patches meet. The vertices are assigned barycentric coordinates ([Section 22.8](#)), which are values that specify a relative location for each point on the desired surface.

The hull shader always outputs a patch, a set of control point locations. However, it can signal that a patch is to be discarded by sending the tessellator an outer tessellation level of zero or less (or not-a-number, NaN). Otherwise, the tessellator generates a mesh and sends it to the domain shader. The control points for the curved surface from the hull shader are used by each invocation of the domain shader to compute the



Figure 3.10. The effect of varying the tessellation factors. The Utah teapot is made of 32 patches. Inner and outer tessellation factors, from left to right, are 1, 2, 4, and 8. (*Images generated by demo from Rideout and Van Gelder [1493].*)

output values for each vertex. The domain shader has a data flow pattern like that of a vertex shader, with each input vertex from the tessellator being processed and generating a corresponding output vertex. The triangles formed are then passed on down the pipeline.

While this system sounds complex, it is structured this way for efficiency, and each shader can be fairly simple. The patch passed into a hull shader will often undergo little or no modification. This shader may also use the patch's estimated distance or screen size to compute tessellation factors on the fly, as for terrain rendering [466]. Alternately, the hull shader may simply pass on a fixed set of values for all patches that the application computes and provides. The tessellator performs an involved but fixed-function process of generating the vertices, giving them positions, and specifying what triangles or lines they form. This data amplification step is performed outside of a shader for computational efficiency [530]. The domain shader takes the barycentric coordinates generated for each point and uses these in the patch's evaluation equation to generate the position, normal, texture coordinates, and other vertex information desired. See [Figure 3.11](#) for an example.

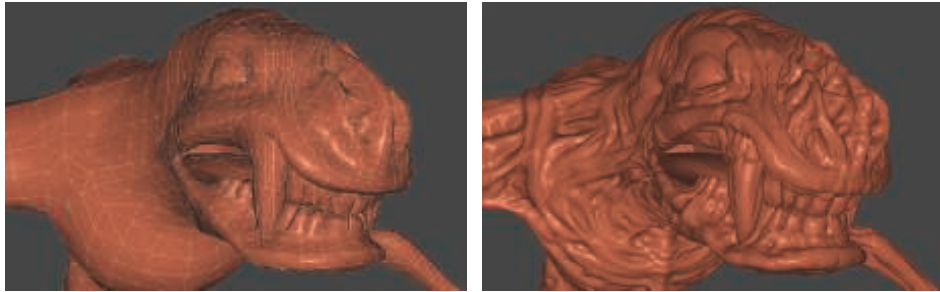


Figure 3.11. On the left is the underlying mesh of about 6000 triangles. On the right, each triangle is tessellated and displaced using PN triangle subdivision. (*Images from NVIDIA SDK 11 [1301] samples, courtesy of NVIDIA Corporation, model from Metro 2033 by 4A Games.*)

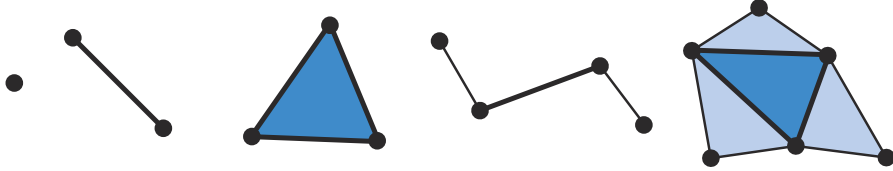


Figure 3.12. Geometry shader input for a geometry shader program is of some single type: point, line segment, triangle. The two rightmost primitives include vertices adjacent to the line and triangle objects. More elaborate patch types are possible.

3.7 The Geometry Shader

The geometry shader can turn primitives into other primitives, something the tessellation stage cannot do. For example, a triangle mesh could be transformed to a wireframe view by having each triangle create line edges. Alternately, the lines could be replaced by quadrilaterals facing the viewer, so making a wireframe rendering with thicker edges [1492]. The geometry shader was added to the hardware-accelerated graphics pipeline with the release of DirectX 10, in late 2006. It is located after the tessellation shader in the pipeline, and its use is optional. While a required part of Shader Model 4.0, it is not used in earlier shader models. OpenGL 3.2 and OpenGL ES 3.2 support this type of shader as well.

The input to the geometry shader is a single object and its associated vertices. The object typically consists of triangles in a strip, a line segment, or simply a point. Extended primitives can be defined and processed by the geometry shader. In particular, three additional vertices outside of a triangle can be passed in, and the two adjacent vertices on a polyline can be used. See [Figure 3.12](#). With DirectX 11 and Shader Model 5.0, you can pass in more elaborate patches, with up to 32 control points. That said, the tessellation stage is more efficient for patch generation [175].

The geometry shader processes this primitive and outputs zero or more vertices, which are treated as points, polylines, or strips of triangles. Note that no output at all can be generated by the geometry shader. In this way, a mesh can be selectively modified by editing vertices, adding new primitives, and removing others.

The geometry shader is designed for modifying incoming data or making a limited number of copies. For example, one use is to generate six transformed copies of data to simultaneously render the six faces of a cube map; see [Section 10.4.3](#). It can also be used to efficiently create cascaded shadow maps for high-quality shadow generation. Other algorithms that take advantage of the geometry shader include creating variable-sized particles from point data, extruding fins along silhouettes for fur rendering, and finding object edges for shadow algorithms. See [Figure 3.13](#) for more examples. These and other uses are discussed throughout the rest of the book.

DirectX 11 added the ability for the geometry shader to use instancing, where the geometry shader can be run a set number of times on any given primitive [530, 1971]. In

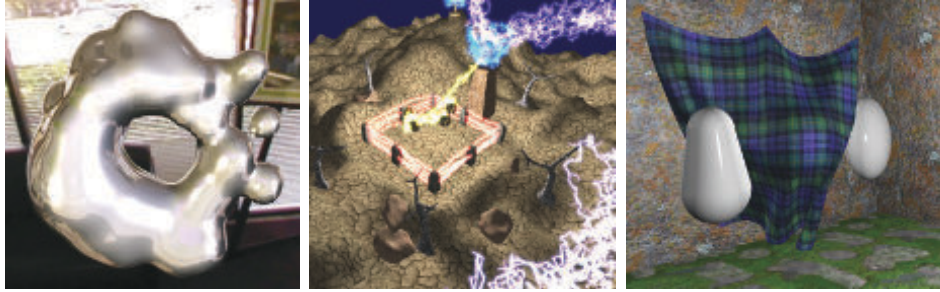


Figure 3.13. Some uses of the geometry shader (GS). On the left, metaball isosurface tessellation is performed on the fly using the GS. In the middle, fractal subdivision of line segments is done using the GS and stream out, and billboards are generated by the GS for display of the lightning. On the right, cloth simulation is performed by using the vertex and geometry shader with stream out. (Images from NVIDIA SDK 10 [1300] samples, courtesy of NVIDIA Corporation.)

OpenGL 4.0 this is specified with an invocation count. The geometry shader can also output up to four *streams*. One stream can be sent on down the rendering pipeline for further processing. All these streams can optionally be sent to stream output render targets.

The geometry shader is guaranteed to output results from primitives in the same order that they are input. This affects performance, because if several shader cores run in parallel, results must be saved and ordered. This and other factors work against the geometry shader being used to replicate or create a large amount of geometry in a single call [175, 530].

After a draw call is issued, there are only three places in the pipeline where work can be created on the GPU: rasterization, the tessellation stage, and the geometry shader. Of these, the geometry shader’s behavior is the least predictable when considering resources and memory needed, since it is fully programmable. In practice the geometry shader usually sees little use, as it does not map well to the GPU’s strengths. On some mobile devices it is implemented in software, so its use is actively discouraged there [69].

3.7.1 Stream Output

The standard use of the GPU’s pipeline is to send data through the vertex shader, then rasterize the resulting triangles and process these in the pixel shader. It used to be that the data always passed through the pipeline and intermediate results could not be accessed. The idea of *stream output* was introduced in Shader Model 4.0. After vertices are processed by the vertex shader (and, optionally, the tessellation and geometry shaders), these can be output in a stream, i.e., an ordered array, in addition to being sent on to the rasterization stage. Rasterization could, in fact, be turned off entirely and the pipeline then used purely as a non-graphical stream processor. Data

processed in this way can be sent back through the pipeline, thus allowing iterative processing. This type of operation can be useful for simulating flowing water or other particle effects, as discussed in [Section 13.8](#). It could also be used to skin a model and then have these vertices available for reuse ([Section 4.4](#)).

Stream output returns data only in the form of floating point numbers, so it can have a noticeable memory cost. Stream output works on primitives, not directly on vertices. If meshes are sent down the pipeline, each triangle generates its own set of three output vertices. Any vertex sharing in the original mesh is lost. For this reason a more typical use is to send just the vertices through the pipeline as a point set primitive. In OpenGL the stream output stage is called *transform feedback*, since the focus of much of its use is transforming vertices and returning them for further processing. Primitives are guaranteed to be sent to the stream output target in the order that they were input, meaning the vertex order will be maintained [[530](#)].

3.8 The Pixel Shader

After the vertex, tessellation, and geometry shaders perform their operations, the primitive is clipped and set up for rasterization, as explained in the previous chapter. This section of the pipeline is relatively fixed in its processing steps, i.e., not programmable but somewhat configurable. Each triangle is traversed to determine which pixels it covers. The rasterizer may also roughly calculate how much the triangle covers each pixel's cell area ([Section 5.4.2](#)). This piece of a triangle partially or fully overlapping the pixel is called a *fragment*.

The values at the triangle's vertices, including the z -value used in the z -buffer, are interpolated across the triangle's surface for each pixel. These values are passed to the *pixel shader*, which then processes the fragment. In OpenGL the pixel shader is known as the *fragment shader*, which is perhaps a better name. We use “pixel shader” throughout this book for consistency. Point and line primitives sent down the pipeline also create fragments for the pixels covered.

The type of interpolation performed across the triangle is specified by the pixel shader program. Normally we use perspective-correct interpolation, so that the world-space distances between pixel surface locations increase as an object recedes in the distance. An example is rendering railroad tracks extending to the horizon. Railroad ties are more closely spaced where the rails are farther away, as more distance is traveled for each successive pixel approaching the horizon. Other interpolation options are available, such as screen-space interpolation, where perspective projection is not taken into account. DirectX 11 gives further control over when and how interpolation is performed [[530](#)].

In programming terms, the vertex shader program's outputs, interpolated across the triangle (or line), effectively become the pixel shader program's inputs. As the GPU has evolved, other inputs have been exposed. For example, the screen position of the fragment is available to the pixel shader in Shader Model 3.0 and beyond. Also,

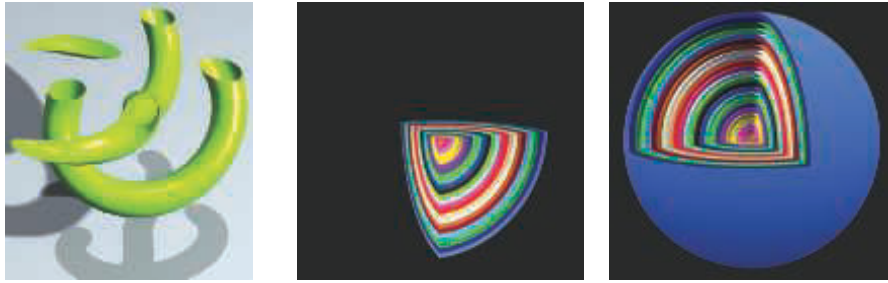


Figure 3.14. User-defined clipping planes. On the left, a single horizontal clipping plane slices the object. In the middle, the nested spheres are clipped by three planes. On the right, the spheres' surfaces are clipped only if they are outside all three clip planes. (*From the three.js examples webgl_clipping and webgl_clipping_intersection [218].*)

which side of a triangle is visible is an input flag. This knowledge is important for rendering a different material on the front versus back of each triangle in a single pass.

With inputs in hand, typically the pixel shader computes and outputs a fragment's color. It can also possibly produce an opacity value and optionally modify its z -depth. During merging, these values are used to modify what is stored at the pixel. The depth value generated in the rasterization stage can also be modified by the pixel shader. The stencil buffer value is usually not modifiable, but rather it is passed through to the merge stage. DirectX 11.3 allows the shader to change this value. Operations such as fog computation and alpha testing have moved from being merge operations to being pixel shader computations in SM 4.0 [175].

A pixel shader also has the unique ability to discard an incoming fragment, i.e., generate no output. One example of how fragment discard can be used is shown in Figure 3.14. Clip plane functionality used to be a configurable element in the fixed-function pipeline and was later specified in the vertex shader. With fragment discard available, this functionality could then be implemented in any way desired in the pixel shader, such as deciding whether clipping volumes should be AND'ed or OR'ed together.

Initially the pixel shader could output to only the merging stage, for eventual display. The number of instructions a pixel shader can execute has grown considerably over time. This increase gave rise to the idea of *multiple render targets* (MRT). Instead of sending results of a pixel shader's program to just the color and z -buffer, multiple sets of values could be generated for each fragment and saved to different buffers, each called a *render target*. Render targets generally have the same x - and y -dimensions; some APIs allow different sizes, but the rendered area will be the smallest of these. Some architectures require render targets to each have the same bit depth, and possibly even identical data formats. Depending on the GPU, the number of render targets available is four or eight.

Even with these limitations, MRT functionality is a powerful aid in performing rendering algorithms more efficiently. A single rendering pass could generate a color image in one target, object identifiers in another, and world-space distances in a third. This ability has also given rise to a different type of rendering pipeline, called *deferred shading*, where visibility and shading are done in separate passes. The first pass stores data about an object’s location and material at each pixel. Successive passes can then efficiently apply illumination and other effects. This class of rendering methods is described in [Section 20.1](#).

The pixel shader’s limitation is that it can normally write to a render target at only the fragment location handed to it, and cannot read current results from neighboring pixels. That is, when a pixel shader program executes, it cannot send its output directly to neighboring pixels, nor can it access others’ recent changes. Rather, it computes results that affect only its own pixel. However, this limitation is not as severe as it sounds. An output image created in one pass can have any of its data accessed by a pixel shader in a later pass. Neighboring pixels can be processed using image processing techniques, described in [Section 12.1](#).

There are exceptions to the rule that a pixel shader cannot know or affect neighboring pixels’ results. One is that the pixel shader can immediately access information for adjacent fragments (albeit indirectly) during the computation of gradient or derivative information. The pixel shader is provided with the amounts by which any interpolated value changes per pixel along the x and y screen axes. Such values are useful for various computations and texture addressing. These gradients are particularly important for operations such as texture filtering ([Section 6.2.2](#)), where we want to know how much of an image covers a pixel. All modern GPUs implement this feature by processing fragments in groups of 2×2 , called a *quad*. When the pixel shader requests a gradient value, the difference between adjacent fragments is returned. See [Figure 3.15](#). A unified core has this capability to access neighboring data—kept in different threads on the same warp—and so can compute gradients for use in the pixel shader. One consequence of this implementation is that gradient information cannot be accessed in parts of the shader affected by dynamic flow control, i.e., an “if” statement or loop with a variable number of iterations. All the fragments in a group must be processed using the same set of instructions so that all four pixels’ results are meaningful for computing gradients. This is a fundamental limitation that exists even in offline rendering systems [64].

DirectX 11 introduced a buffer type that allows write access to any location, the *unordered access view* (UAV). Originally for only pixel and compute shaders, access to UAVs was extended to all shaders in DirectX 11.1 [146]. OpenGL 4.3 calls this a *shader storage buffer object* (SSBO). Both names are descriptive in their own way. Pixel shaders are run in parallel, in an arbitrary order, and this storage buffer is shared among them.

Often some mechanism is needed to avoid a *data race condition* (a.k.a. a *data hazard*), where both shader programs are “racing” to influence the same value, possibly

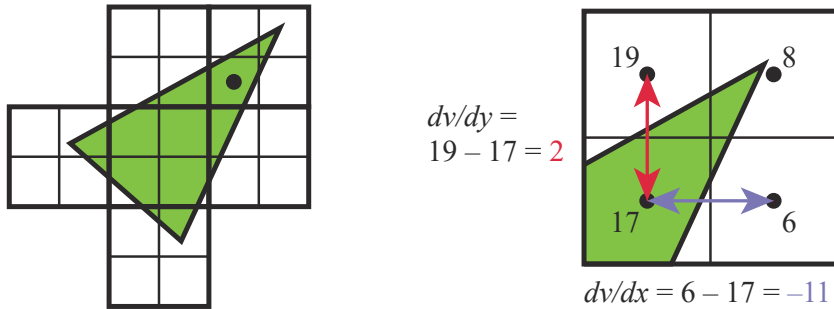


Figure 3.15. On the left, a triangle is rasterized into quads, sets of 2×2 pixels. The gradient computations for the pixel marked with a black dot is then shown on the right. The value for v is shown for each of the four pixel locations in the quad. Note how three of the pixels are not covered by the triangle, yet they are still processed by the GPU so that the gradients can be found. The gradients in the x and y screen directions are computed for the lower left pixel by using its two quad neighbors.

leading to arbitrary results. As an example, an error could occur if two invocations of a pixel shader tried to, say, add to the same retrieved value at about the same time. Both would retrieve the original value, both would modify it locally, but then whichever invocation wrote its result last would wipe out the contribution of the other invocation—only one addition would occur. GPUs avoid this problem by having dedicated atomic units that the shader can access [530]. However, atomics mean that some shaders may stall as they wait to access a memory location undergoing read/modify/write by another shader.

While atomics avoid data hazards, many algorithms require a specific order of execution. For example, you may want to draw a more distant transparent blue triangle before overlaying it with a red transparent triangle, blending the red atop the blue. It is possible for a pixel to have two pixel shader invocations for a pixel, one for each triangle, executing in such a way that the red triangle’s shader completes before the blue’s. In the standard pipeline, the fragment results are sorted in the merger stage before being processed. *Rasterizer order views* (ROVs) were introduced in DirectX 11.3 to enforce an order of execution. These are like UAVs; they can be read and written by shaders in the same fashion. The key difference is that ROVs guarantee that the data are accessed in the proper order. This increases the usefulness of these shader-accessible buffers considerably [327, 328]. For example, ROVs make it possible for the pixel shader to write its own blending methods, since it can directly access and write to any location in the ROV, and thus no merging stage is needed [176]. The price is that, if an out-of-order access is detected, a pixel shader invocation may stall until triangles drawn earlier are processed.

3.9 The Merging Stage

As discussed in [Section 2.5.2](#), the merging stage is where the depths and colors of the individual fragments (generated in the pixel shader) are combined with the framebuffer. DirectX calls this stage the *output merger*; OpenGL refers to it as *per-sample operations*. On most traditional pipeline diagrams (including our own), this stage is where stencil-buffer and *z*-buffer operations occur. If the fragment is visible, another operation that takes place in this stage is color blending. For opaque surfaces there is no real blending involved, as the fragment's color simply replaces the previously stored color. Actual blending of the fragment and stored color is commonly used for transparency and compositing operations ([Section 5.5](#)).

Imagine that a fragment generated by rasterization is run through the pixel shader and then is found to be hidden by some previously rendered fragment when the *z*-buffer is applied. All the processing done in the pixel shader was then unnecessary. To avoid this waste, many GPUs perform some merge testing before the pixel shader is executed [530]. The fragment's *z*-depth (and whatever else is in use, such as the stencil buffer or scissoring) is used for testing visibility. The fragment is culled if hidden. This functionality is called *early-z* [1220, 1542]. The pixel shader has the ability to change the *z*-depth of the fragment or to discard the fragment entirely. If either type of operation is found to exist in a pixel shader program, *early-z* then generally cannot be used and is turned off, usually making the pipeline less efficient. DirectX 11 and OpenGL 4.2 allow the pixel shader to force *early-z* testing to be on, though with a number of limitations [530]. See [Section 23.7](#) for more about *early-z* and other *z*-buffer optimizations. Using *early-z* effectively can have a large effect on performance, which is discussed in detail in [Section 18.4.5](#).

The merging stage occupies the middle ground between fixed-function stages, such as triangle setup, and the fully programmable shader stages. Although it is not programmable, its operation is highly configurable. Color blending in particular can be set up to perform a large number of different operations. The most common are combinations of multiplication, addition, and subtraction involving the color and alpha values, but other operations are possible, such as minimum and maximum, as well as bitwise logic operations. DirectX 10 added the capability to blend two colors from the pixel shader with the framebuffer color. This capability is called *dual source-color blending* and cannot be used in conjunction with multiple render targets. MRT does otherwise support blending, and DirectX 10.1 introduced the capability to perform different blend operations on each separate buffer.

As mentioned at the end of the previous section, DirectX 11.3 provided a way to make blending programmable through ROVs, though at a price in performance. ROVs and the merging stage both guarantee draw order, a.k.a. output invariance. Regardless of the order in which pixel shader results are generated, it is an API requirement that results are sorted and sent to the merging stage in the order in which they are input, object by object and triangle by triangle.

3.10 The Compute Shader

The GPU can be used for more than implementing the traditional graphics pipeline. There are many non-graphical uses in fields as varied as computing the estimated value of stock options and training neural nets for deep learning. Using hardware in this way is called *GPU computing*. Platforms such as CUDA and OpenCL are used to control the GPU as a massive parallel processor, with no real need or access to graphics-specific functionality. These frameworks often use languages such as C or C++ with extensions, along with libraries made for the GPU.

Introduced in DirectX 11, the *compute shader* is a form of GPU computing, in that it is a shader that is not locked into a location in the graphics pipeline. It is closely tied to the process of rendering in that it is invoked by the graphics API. It is used alongside vertex, pixel, and other shaders. It draws upon the same pool of unified shader processors as those used in the pipeline. It is a shader like the others, in that it has some set of input data and can access buffers (such as textures) for input and output. Warps and threads are more visible in a compute shader. For example, each invocation gets a thread index that it can access. There is also the concept of a *thread group*, which consists of 1 to 1024 threads in DirectX 11. These thread groups are specified by x -, y -, and z -coordinates, mostly for simplicity of use in shader code. Each thread group has a small amount of memory that is shared among threads. In DirectX 11, this amounts to 32 kB. Compute shaders are executed by thread group, so that all threads in the group are guaranteed to run concurrently [1971].

One important advantage of compute shaders is that they can access data generated on the GPU. Sending data from the GPU to the CPU incurs a delay, so performance can be improved if processing and results can be kept resident on the GPU [1403]. Post-processing, where a rendered image is modified in some way, is a common use of compute shaders. The shared memory means that intermediate results from sampling image pixels can be shared with neighboring threads. Using a compute shader to determine the distribution or average luminance of an image, for example, has been found to run twice as fast as performing this operation on a pixel shader [530].

Compute shaders are also useful for particle systems, mesh processing such as facial animation [134], culling [1883, 1884], image filtering [1102, 1710], improving depth precision [991], shadows [865], depth of field [764], and any other tasks where a set of GPU processors can be brought to bear. Wihlidal [1884] discusses how compute shaders can be more efficient than tessellation hull shaders. See Figure 3.16 for other uses.

This ends our review of the GPU's implementation of the rendering pipeline. There are many ways in which the GPUs functions can be used and combined to perform various rendering-related processes. Relevant theory and algorithms tuned to take advantage of these capabilities are the central subjects of this book. Our focus now moves on to transforms and shading.



Figure 3.16. Compute shader examples. On the left, a compute shader is used to simulate hair affected by wind, with the hair itself rendered using the tessellation stage. In the middle, a compute shader performs a rapid blur operation. On the right, ocean waves are simulated. (*Images from NVIDIA SDK 11 [1301] samples, courtesy of NVIDIA Corporation.*)

Further Reading and Resources

Giesen’s tour of the graphics pipeline [530] discusses many facets of the GPU at length, explaining why elements work the way they do. The course by Fatahalian and Bryant [462] discusses GPU parallelism in a series of detailed lecture slide sets. While focused on GPU computing using CUDA, the introductory part of Kirk and Hwa’s book [903] discusses the evolution and design philosophy for the GPU.

To learn the formal aspects of shader programming takes some work. Books such as the *OpenGL Superbible* [1606] and *OpenGL Programming Guide* [885] include material on shader programming. The older book *OpenGL Shading Language* [1512] does not cover more recent shader stages, such as the geometry and tessellation shaders, but does focus specifically on shader-related algorithms. See this book’s website, realtimerendering.com, for recent and recommended books.



Taylor & Francis
Taylor & Francis Group
<http://taylorandfrancis.com>

Chapter 4

Transforms

*“What if angry vectors veer
Round your sleeping head, and form.
There’s never need to fear
Violence of the poor world’s abstract storm.”*

—Robert Penn Warren

A *transform* is an operation that takes entities such as points, vectors, or colors and converts them in some way. For the computer graphics practitioner, it is extremely important to master transforms. With them, you can position, reshape, and animate objects, lights, and cameras. You can also ensure that all computations are carried out in the same coordinate system, and project objects onto a plane in different ways. These are only a few of the operations that can be performed with transforms, but they are sufficient to demonstrate the importance of the transform’s role in real-time graphics, or, for that matter, in any kind of computer graphics.

A *linear transform* is one that preserves vector addition and scalar multiplication. Specifically,

$$\mathbf{f}(\mathbf{x}) + \mathbf{f}(\mathbf{y}) = \mathbf{f}(\mathbf{x} + \mathbf{y}), \quad (4.1)$$

$$k\mathbf{f}(\mathbf{x}) = \mathbf{f}(k\mathbf{x}). \quad (4.2)$$

As an example, $\mathbf{f}(\mathbf{x}) = 5\mathbf{x}$ is a transform that takes a vector and multiplies each element by five. To prove that this is linear, the two conditions ([Equations 4.1](#) and [4.2](#)) need to be fulfilled. The first condition holds since any two vectors multiplied by five and then added will be the same as adding the vectors and then multiplying. The scalar multiplication condition ([Equation 4.2](#)) is clearly fulfilled. This function is called a scaling transform, as it changes the scale (size) of an object. The rotation transform is another linear transform that rotates a vector about the origin. Scaling and rotation transforms, in fact all linear transforms for three-element vectors, can be represented using a 3×3 matrix.

However, this size of matrix is usually not large enough. A function for a three-element vector \mathbf{x} such as $\mathbf{f}(\mathbf{x}) = \mathbf{x} + (7, 3, 2)$ is not linear. Performing this function on two separate vectors will add each value of $(7, 3, 2)$ twice to form the result. Adding a fixed vector to another vector performs a translation, e.g., it moves all locations by

the same amount. This is a useful type of transform, and we would like to combine various transforms, e.g., scale an object to be half as large, then move it to a different location. Keeping functions in the simple forms used so far makes it difficult to easily combine them.

Combining linear transforms and translations can be done using an *affine transform*, typically stored as a 4×4 matrix. An affine transform is one that performs a linear transform and then a translation. To represent four-element vectors we use *homogeneous notation*, denoting points and directions in the same way (using bold lowercase letters). A direction vector is represented as $\mathbf{v} = (v_x \ v_y \ v_z \ 0)^T$ and a point as $\mathbf{v} = (v_x \ v_y \ v_z \ 1)^T$. Throughout the chapter, we will make extensive use of the terminology and operations explained in the downloadable linear algebra appendix, found on realtimerendering.com.

All translation, rotation, scaling, reflection, and shearing matrices are affine. The main characteristic of an affine matrix is that it preserves the parallelism of lines, but not necessarily lengths and angles. An affine transform may also be any sequence of concatenations of individual affine transforms.

This chapter will begin with the most essential, basic affine transforms. This section can be seen as a “reference manual” for simple transforms. More specialized matrices are then described, followed by a discussion and description of quaternions, a powerful transform tool. Then follows vertex blending and morphing, which are two simple but effective ways of expressing animations of meshes. Finally, projection matrices are described. Most of these transforms, their notations, functions, and properties are summarized in [Table 4.1](#), where an orthogonal matrix is one whose inverse is the transpose.

Transforms are a basic tool for manipulating geometry. Most graphics application programming interfaces let the user set arbitrary matrices, and sometimes a library may be used with matrix operations that implement many of the transforms discussed in this chapter. However, it is still worthwhile to understand the real matrices and their interaction behind the function calls. Knowing what the matrix does after such a function call is a start, but understanding the properties of the matrix itself will take you further. For example, such an understanding enables you to discern when you are dealing with an orthogonal matrix, whose inverse is its transpose, making for faster matrix inversions. Knowledge like this can lead to accelerated code.

4.1 Basic Transforms

This section describes the most basic transforms, such as translation, rotation, scaling, shearing, transform concatenation, the rigid-body transform, normal transform (which is not so normal), and computation of inverses. For the experienced reader, this can be used as a reference manual for simple transforms, and for the novice, it can serve as an introduction to the subject. This material is necessary background for the rest of this chapter and for other chapters in this book. We start with the simplest of transforms—the translation.

Notation	Name	Characteristics
$\mathbf{T}(\mathbf{t})$	translation matrix	Moves a point. Affine.
$\mathbf{R}_x(\rho)$	rotation matrix	Rotates ρ radians around the x -axis. Similar notation for the y - and z -axes. Orthogonal & affine.
\mathbf{R}	rotation matrix	Any rotation matrix. Orthogonal & affine.
$\mathbf{S}(\mathbf{s})$	scaling matrix	Scales along all x -, y -, and z -axes according to \mathbf{s} . Affine.
$\mathbf{H}_{ij}(s)$	shear matrix	Shears component i by a factor s , with respect to component j . $i, j \in \{x, y, z\}$. Affine.
$\mathbf{E}(h, p, r)$	Euler transform	Orientation matrix given by the Euler angles head (yaw), pitch, roll. Orthogonal & affine.
$\mathbf{P}_o(s)$	orthographic projection	Parallel projects onto some plane or to a volume. Affine.
$\mathbf{P}_p(s)$	perspective projection	Projects with perspective onto a plane or to a volume.
$\text{slerp}(\hat{\mathbf{q}}, \hat{\mathbf{r}}, t)$	slerp transform	Creates an interpolated quaternion with respect to the quaternions $\hat{\mathbf{q}}$ and $\hat{\mathbf{r}}$, and the parameter t .

Table 4.1. Summary of most of the transforms discussed in this chapter.

4.1.1 Translation

A change from one location to another is represented by a translation matrix, \mathbf{T} . This matrix translates an entity by a vector $\mathbf{t} = (t_x, t_y, t_z)$. \mathbf{T} is given below by Equation 4.3:

$$\mathbf{T}(\mathbf{t}) = \mathbf{T}(t_x, t_y, t_z) = \begin{pmatrix} 1 & 0 & 0 & t_x \\ 0 & 1 & 0 & t_y \\ 0 & 0 & 1 & t_z \\ 0 & 0 & 0 & 1 \end{pmatrix}. \quad (4.3)$$

An example of the effect of the translation transform is shown in Figure 4.1. It is easily shown that the multiplication of a point $\mathbf{p} = (p_x, p_y, p_z, 1)$ with $\mathbf{T}(\mathbf{t})$ yields a new point $\mathbf{p}' = (p_x + t_x, p_y + t_y, p_z + t_z, 1)$, which is clearly a translation. Notice that a vector $\mathbf{v} = (v_x, v_y, v_z, 0)$ is left unaffected by a multiplication by \mathbf{T} , because a direction vector cannot be translated. In contrast, both points and vectors are affected by the rest of the affine transforms. The inverse of a translation matrix is $\mathbf{T}^{-1}(\mathbf{t}) = \mathbf{T}(-\mathbf{t})$, that is, the vector \mathbf{t} is negated.

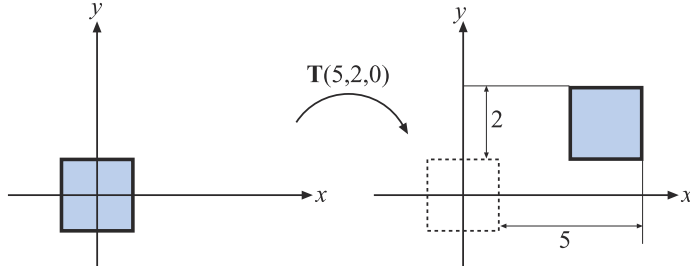


Figure 4.1. The square on the left is transformed with a translation matrix $\mathbf{T}(5, 2, 0)$, whereby the square is moved 5 distance units to the right and 2 upward.

We should mention at this point that another valid notational scheme sometimes seen in computer graphics uses matrices with translation vectors in the bottom row. For example, DirectX uses this form. In this scheme, the order of matrices would be reversed, i.e., the order of application would read from left to right. Vectors and matrices in this notation are said to be in *row-major* form since the vectors are rows. In this book, we use *column-major* form. Whichever is used, this is purely a notational difference. When the matrix is stored in memory, the last four values of the sixteen are the three translation values followed by a one.

4.1.2 Rotation

A rotation transform rotates a vector (position or direction) by a given angle around a given axis passing through the origin. Like a translation matrix, it is a *rigid-body transform*, i.e., it preserves the distances between points transformed, and preserves handedness (i.e., it never causes left and right to swap sides). These two types of transforms are clearly useful in computer graphics for positioning and orienting objects. An *orientation matrix* is a rotation matrix associated with a camera view or object that defines its orientation in space, i.e., its directions for up and forward.

In two dimensions, the rotation matrix is simple to derive. Assume that we have a vector, $\mathbf{v} = (v_x, v_y)$, which we parameterize as $\mathbf{v} = (v_x, v_y) = (r \cos \theta, r \sin \theta)$. If we were to rotate that vector by ϕ radians (counterclockwise), then we would get $\mathbf{u} = (r \cos(\theta + \phi), r \sin(\theta + \phi))$. This can be rewritten as

$$\begin{aligned}\mathbf{u} &= \begin{pmatrix} r \cos(\theta + \phi) \\ r \sin(\theta + \phi) \end{pmatrix} = \begin{pmatrix} r(\cos \theta \cos \phi - \sin \theta \sin \phi) \\ r(\sin \theta \cos \phi + \cos \theta \sin \phi) \end{pmatrix} \\ &= \underbrace{\begin{pmatrix} \cos \phi & -\sin \phi \\ \sin \phi & \cos \phi \end{pmatrix}}_{\mathbf{R}(\phi)} \underbrace{\begin{pmatrix} r \cos \theta \\ r \sin \theta \end{pmatrix}}_{\mathbf{v}} = \mathbf{R}(\phi)\mathbf{v},\end{aligned}\tag{4.4}$$

where we used the angle sum relation to expand $\cos(\theta + \phi)$ and $\sin(\theta + \phi)$. In three dimensions, commonly used rotation matrices are $\mathbf{R}_x(\phi)$, $\mathbf{R}_y(\phi)$, and $\mathbf{R}_z(\phi)$, which

rotate an entity ϕ radians around the x -, y -, and z -axes, respectively. They are given by Equations 4.5–4.7:

$$\mathbf{R}_x(\phi) = \begin{pmatrix} 1 & 0 & 0 & 0 \\ 0 & \cos \phi & -\sin \phi & 0 \\ 0 & \sin \phi & \cos \phi & 0 \\ 0 & 0 & 0 & 1 \end{pmatrix}, \quad (4.5)$$

$$\mathbf{R}_y(\phi) = \begin{pmatrix} \cos \phi & 0 & \sin \phi & 0 \\ 0 & 1 & 0 & 0 \\ -\sin \phi & 0 & \cos \phi & 0 \\ 0 & 0 & 0 & 1 \end{pmatrix}, \quad (4.6)$$

$$\mathbf{R}_z(\phi) = \begin{pmatrix} \cos \phi & -\sin \phi & 0 & 0 \\ \sin \phi & \cos \phi & 0 & 0 \\ 0 & 0 & 1 & 0 \\ 0 & 0 & 0 & 1 \end{pmatrix}. \quad (4.7)$$

If the bottom row and rightmost column are deleted from a 4×4 matrix, a 3×3 matrix is obtained. For every 3×3 rotation matrix, \mathbf{R} , that rotates ϕ radians around any axis, the trace (which is the sum of the diagonal elements in a matrix) is constant independent of the axis, and is computed as [997]:

$$\text{tr}(\mathbf{R}) = 1 + 2 \cos \phi. \quad (4.8)$$

The effect of a rotation matrix may be seen in Figure 4.4 on page 65. What characterizes a rotation matrix, $\mathbf{R}_i(\phi)$, besides the fact that it rotates ϕ radians around axis i , is that it leaves all points on the rotation axis, i , unchanged. Note that \mathbf{R} will also be used to denote a rotation matrix around any axis. The axis rotation matrices given above can be used in a series of three transforms to perform any arbitrary axis rotation. This procedure is discussed in Section 4.2.1. Performing a rotation around an arbitrary axis directly is covered in Section 4.2.4.

All rotation matrices have a determinant of one and are orthogonal. This also holds for concatenations of any number of these transforms. There is another way to obtain the inverse: $\mathbf{R}_i^{-1}(\phi) = \mathbf{R}_i(-\phi)$, i.e., rotate in the opposite direction around the same axis.

EXAMPLE: ROTATION AROUND A POINT. Assume that we want to rotate an object by ϕ radians around the z -axis, with the center of rotation being a certain point, \mathbf{p} . What is the transform? This scenario is depicted in Figure 4.2. Since a rotation around a point is characterized by the fact that the point itself is unaffected by the rotation, the transform starts by translating the object so that \mathbf{p} coincides with the origin, which is done with $\mathbf{T}(-\mathbf{p})$. Thereafter follows the actual rotation: $\mathbf{R}_z(\phi)$. Finally, the object has to be translated back to its original position using $\mathbf{T}(\mathbf{p})$. The resulting transform, \mathbf{X} , is then given by

$$\mathbf{X} = \mathbf{T}(\mathbf{p})\mathbf{R}_z(\phi)\mathbf{T}(-\mathbf{p}). \quad (4.9)$$

Note the order of the matrices above. □

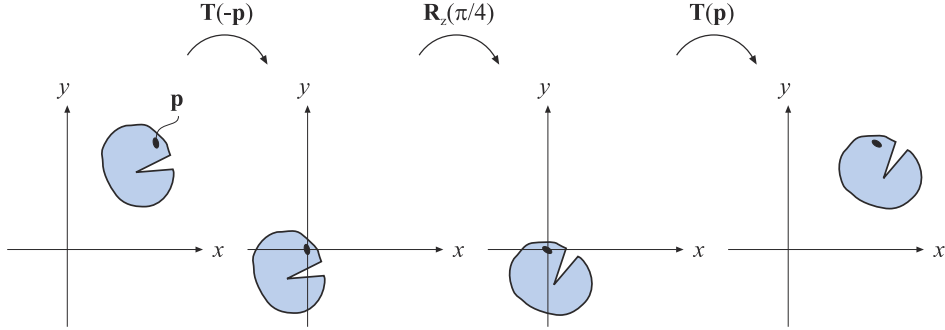


Figure 4.2. Example of rotation around a specific point \mathbf{p} .

4.1.3 Scaling

A scaling matrix, $\mathbf{S}(\mathbf{s}) = \mathbf{S}(s_x, s_y, s_z)$, scales an entity with factors s_x , s_y , and s_z along the x -, y -, and z -directions, respectively. This means that a scaling matrix can be used to enlarge or diminish an object. The larger the s_i , $i \in \{x, y, z\}$, the larger the scaled entity gets in that direction. Setting any of the components of \mathbf{s} to 1 naturally avoids a change in scaling in that direction. [Equation 4.10](#) shows \mathbf{S} :

$$\mathbf{S}(\mathbf{s}) = \begin{pmatrix} s_x & 0 & 0 & 0 \\ 0 & s_y & 0 & 0 \\ 0 & 0 & s_z & 0 \\ 0 & 0 & 0 & 1 \end{pmatrix}. \quad (4.10)$$

[Figure 4.4](#) on page 65 illustrates the effect of a scaling matrix. The scaling operation is called *uniform* if $s_x = s_y = s_z$ and *nonuniform* otherwise. Sometimes the terms *isotropic* and *anisotropic* scaling are used instead of uniform and nonuniform. The inverse is $\mathbf{S}^{-1}(\mathbf{s}) = \mathbf{S}(1/s_x, 1/s_y, 1/s_z)$.

Using homogeneous coordinates, another valid way to create a uniform scaling matrix is by manipulating matrix element at position (3, 3), i.e., the element at the lower right corner. This value affects the w -component of the homogeneous coordinate, and so scales every coordinate of a point (not direction vectors) transformed by the matrix. For example, to scale uniformly by a factor of 5, the elements at (0, 0), (1, 1), and (2, 2) in the scaling matrix can be set to 5, or the element at (3, 3) can be set to 1/5. The two different matrices for performing this are shown below:

$$\mathbf{S} = \begin{pmatrix} 5 & 0 & 0 & 0 \\ 0 & 5 & 0 & 0 \\ 0 & 0 & 5 & 0 \\ 0 & 0 & 0 & 1 \end{pmatrix}, \quad \mathbf{S}' = \begin{pmatrix} 1 & 0 & 0 & 0 \\ 0 & 1 & 0 & 0 \\ 0 & 0 & 1 & 0 \\ 0 & 0 & 0 & 1/5 \end{pmatrix}. \quad (4.11)$$

In contrast to using \mathbf{S} for uniform scaling, using \mathbf{S}' must always be followed by homogenization. This may be inefficient, since it involves divides in the homogenization

process; if the element at the lower right (position $(3, 3)$) is 1, no divides are necessary. Of course, if the system always does this division without testing for 1, then there is no extra cost.

A negative value on one or three of the components of \mathbf{s} gives a type of *reflection matrix*, also called a *mirror matrix*. If only two scale factors are -1 , then we will rotate π radians. It should be noted that a rotation matrix concatenated with a reflection matrix is also a reflection matrix. Hence, the following is a reflection matrix:

$$\underbrace{\begin{pmatrix} \cos(\pi/2) & \sin(\pi/2) \\ -\sin(\pi/2) & \cos(\pi/2) \end{pmatrix}}_{\text{rotation}} \underbrace{\begin{pmatrix} 1 & 0 \\ 0 & -1 \end{pmatrix}}_{\text{reflection}} = \begin{pmatrix} 0 & -1 \\ -1 & 0 \end{pmatrix}. \quad (4.12)$$

Reflection matrices usually require special treatment when detected. For example, a triangle with vertices in a counterclockwise order will get a clockwise order when transformed by a reflection matrix. This order change can cause incorrect lighting and backface culling to occur. To detect whether a given matrix reflects in some manner, compute the determinant of the upper left 3×3 elements of the matrix. If the value is negative, the matrix is reflective. For example, the determinant of the matrix in [Equation 4.12](#) is $0 \cdot 0 - (-1) \cdot (-1) = -1$.

EXAMPLE: SCALING IN A CERTAIN DIRECTION. The scaling matrix \mathbf{S} scales along only the x -, y -, and z -axes. If scaling should be performed in other directions, a compound transform is needed. Assume that scaling should be done along the axes of the orthonormal, right-oriented vectors \mathbf{f}^x , \mathbf{f}^y , and \mathbf{f}^z . First, construct the matrix \mathbf{F} , to change the basis, as below:

$$\mathbf{F} = \begin{pmatrix} \mathbf{f}^x & \mathbf{f}^y & \mathbf{f}^z & \mathbf{0} \\ 0 & 0 & 0 & 1 \end{pmatrix}. \quad (4.13)$$

The idea is to make the coordinate system given by the three axes coincide with the standard axes, then use the standard scaling matrix, and then transform back. The first step is carried out by multiplying with the transpose, i.e., the inverse, of \mathbf{F} . Then the actual scaling is done, followed by a transform back. The transform is shown in [Equation 4.14](#):

$$\mathbf{X} = \mathbf{F}\mathbf{S}(\mathbf{s})\mathbf{F}^T. \quad (4.14)$$

□

4.1.4 Shearing

Another class of transforms is the set of shearing matrices. These can, for example, be used in games to distort an entire scene to create a psychedelic effect or otherwise warp a model's appearance. There are six basic shearing matrices, and they are denoted $\mathbf{H}_{xy}(s)$, $\mathbf{H}_{xz}(s)$, $\mathbf{H}_{yx}(s)$, $\mathbf{H}_{yz}(s)$, $\mathbf{H}_{zx}(s)$, and $\mathbf{H}_{zy}(s)$. The first subscript is used to denote which coordinate is being changed by the shear matrix, while the second

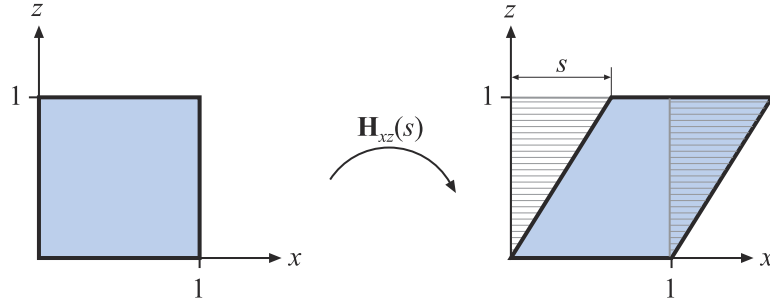


Figure 4.3. The effect of shearing the unit square with $\mathbf{H}_{xz}(s)$. Both the y - and z -values are unaffected by the transform, while the x -value is the sum of the old x -value and s multiplied by the z -value, causing the square to become slanted. This transform is area-preserving, which can be seen in that the dashed areas are the same.

subscript indicates the coordinate which does the shearing. An example of a shear matrix, $\mathbf{H}_{xz}(s)$, is shown in [Equation 4.15](#). Observe that the subscript can be used to find the position of the parameter s in the matrix below; the x (whose numeric index is 0) identifies row zero, and the z (whose numeric index is 2) identifies column two, and so the s is located there:

$$\mathbf{H}_{xz}(s) = \begin{pmatrix} 1 & 0 & s & 0 \\ 0 & 1 & 0 & 0 \\ 0 & 0 & 1 & 0 \\ 0 & 0 & 0 & 1 \end{pmatrix}. \quad (4.15)$$

The effect of multiplying this matrix with a point \mathbf{p} yields a point: $(p_x + sp_z \ p_y \ p_z)^T$. Graphically, this is shown for the unit square in [Figure 4.3](#). The inverse of $\mathbf{H}_{ij}(s)$ (shearing the i th coordinate with respect to the j th coordinate, where $i \neq j$), is generated by shearing in the opposite direction, that is, $\mathbf{H}_{ij}^{-1}(s) = \mathbf{H}_{ij}(-s)$.

You can also use a slightly different kind of shear matrix:

$$\mathbf{H}'_{xy}(s, t) = \begin{pmatrix} 1 & 0 & s & 0 \\ 0 & 1 & t & 0 \\ 0 & 0 & 1 & 0 \\ 0 & 0 & 0 & 1 \end{pmatrix}. \quad (4.16)$$

Here, however, both subscripts are used to denote that these coordinates are to be sheared by the third coordinate. The connection between these two different kinds of descriptions is $\mathbf{H}'_{ij}(s, t) = \mathbf{H}_{ik}(s)\mathbf{H}_{jk}(t)$, where k is used as an index to the third coordinate. The right matrix to use is a matter of taste. Finally, it should be noted that since the determinant of any shear matrix $|\mathbf{H}| = 1$, this is a volume-preserving transformation, which also is illustrated in [Figure 4.3](#).

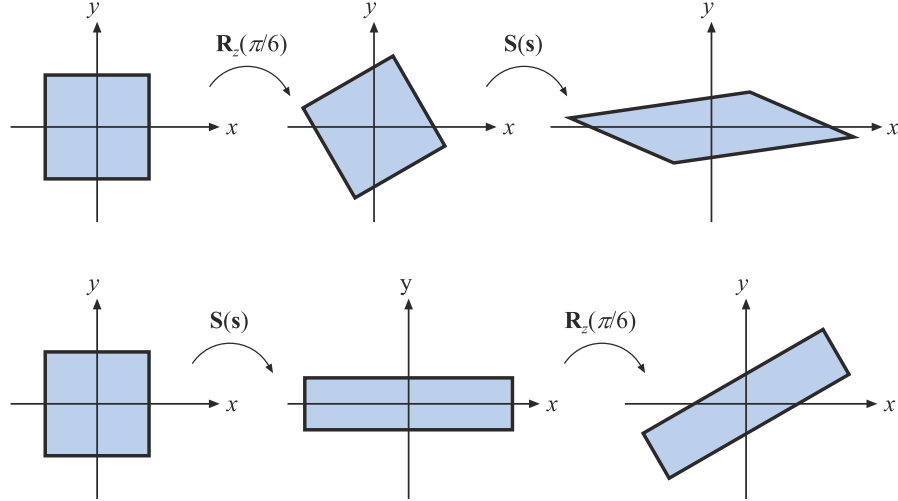


Figure 4.4. This illustrates the order dependency when multiplying matrices. In the top row, the rotation matrix $R_z(\pi/6)$ is applied followed by a scaling, $S(s)$, where $s = (2, 0.5, 1)$. The composite matrix is then $S(s)R_z(\pi/6)$. In the bottom row, the matrices are applied in the reverse order, yielding $R_z(\pi/6)S(s)$. The results are clearly different. It generally holds that $MN \neq NM$, for arbitrary matrices M and N .

4.1.5 Concatenation of Transforms

Due to the noncommutativity of the multiplication operation on matrices, the order in which the matrices occur matters. Concatenation of transforms is therefore said to be order-dependent.

As an example of order dependency, consider two matrices, \mathbf{S} and \mathbf{R} . $\mathbf{S}(2, 0.5, 1)$ scales the x -component by a factor two and the y -component by a factor 0.5. $\mathbf{R}_z(\pi/6)$ rotates $\pi/6$ radians counterclockwise around the z -axis (which points outward from page of this book in a right-handed coordinate system). These matrices can be multiplied in two ways, with the results being entirely different. The two cases are shown in Figure 4.4.

The obvious reason to concatenate a sequence of matrices into a single one is to gain efficiency. For example, imagine that you have a game scene that has several million vertices, and that all objects in the scene must be scaled, rotated, and finally translated. Now, instead of multiplying all vertices with each of the three matrices, the three matrices are concatenated into a single matrix. This single matrix is then applied to the vertices. This composite matrix is $\mathbf{C} = \mathbf{TRS}$. Note the order here. The scaling matrix, \mathbf{S} , should be applied to the vertices first, and therefore appears to the right in the composition. This ordering implies that $\mathbf{TRSp} = (\mathbf{T}(\mathbf{R}(\mathbf{Sp})))$, where \mathbf{p} is a point to be transformed. Incidentally, \mathbf{TRS} is the order commonly used by scene graph systems.

It is worth noting that while matrix concatenation is order-dependent, the matrices can be grouped as desired. For example, say that with \mathbf{TRSp} you would like to compute the rigid-body motion transform \mathbf{TR} once. It is valid to group these two matrices together, $(\mathbf{TR})(\mathbf{Sp})$, and replace with the intermediate result. Thus, matrix concatenation is *associative*.

4.1.6 The Rigid-Body Transform

When a person grabs a solid object, say a pen from a table, and moves it to another location, perhaps to a shirt pocket, only the object's orientation and location change, while the shape of the object generally is not affected. Such a transform, consisting of concatenations of only translations and rotations, is called a rigid-body transform. It has the characteristic of preserving lengths, angles, and handedness.

Any rigid-body matrix, \mathbf{X} , can be written as the concatenation of a translation matrix, $\mathbf{T}(\mathbf{t})$, and a rotation matrix, \mathbf{R} . Thus, \mathbf{X} has the appearance of the matrix in [Equation 4.17](#):

$$\mathbf{X} = \mathbf{T}(\mathbf{t})\mathbf{R} = \begin{pmatrix} r_{00} & r_{01} & r_{02} & t_x \\ r_{10} & r_{11} & r_{12} & t_y \\ r_{20} & r_{21} & r_{22} & t_z \\ 0 & 0 & 0 & 1 \end{pmatrix}. \quad (4.17)$$

The inverse of \mathbf{X} is computed as $\mathbf{X}^{-1} = (\mathbf{T}(\mathbf{t})\mathbf{R})^{-1} = \mathbf{R}^{-1}\mathbf{T}(\mathbf{t})^{-1} = \mathbf{R}^T\mathbf{T}(-\mathbf{t})$. Thus, to compute the inverse, the upper left 3×3 matrix of \mathbf{R} is transposed, and the translation values of \mathbf{T} change sign. These two new matrices are multiplied together in opposite order to obtain the inverse. Another way to compute the inverse of \mathbf{X} is to consider \mathbf{R} (making \mathbf{R} appear as 3×3 matrix) and \mathbf{X} in the following notation (notation described on page 6 with [Equation 1.2](#)):

$$\bar{\mathbf{R}} = (\mathbf{r}_{,0} \quad \mathbf{r}_{,1} \quad \mathbf{r}_{,2}) = \begin{pmatrix} \mathbf{r}_0^T \\ \mathbf{r}_1^T \\ \mathbf{r}_2^T \end{pmatrix}, \quad (4.18)$$

$$\mathbf{X} = \begin{pmatrix} \bar{\mathbf{R}} & \mathbf{t} \\ \mathbf{0}^T & 1 \end{pmatrix},$$

where $\mathbf{r}_{,0}$ means the first column of the rotation matrix (i.e., the comma indicates any value from 0 to 2, while the second subscript is 0) and \mathbf{r}_0^T is the first row of the column matrix. Note that $\mathbf{0}$ is a 3×1 column vector filled with zeros. Some calculations yield the inverse in the expression shown in [Equation 4.19](#):

$$\mathbf{X}^{-1} = \begin{pmatrix} \mathbf{r}_0 & \mathbf{r}_1 & \mathbf{r}_2 & -\bar{\mathbf{R}}^T\mathbf{t} \\ 0 & 0 & 0 & 1 \end{pmatrix}. \quad (4.19)$$

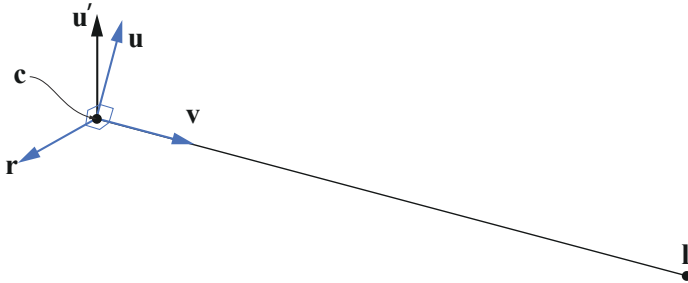


Figure 4.5. The geometry involved in computing a transform that orients the camera at \mathbf{c} , with up vector \mathbf{u}' , to look at the point \mathbf{l} . For that purpose, we need to compute \mathbf{r} , \mathbf{u} , and \mathbf{v} .

EXAMPLE: ORIENTING THE CAMERA. A common task in graphics is to orient the camera so that it looks at a certain position. Here we will present what `gluLookAt()` (from the OpenGL Utility Library, GLU for short) does. Even though this function call itself is not used much nowadays, the task remains common. Assume that the camera is located at \mathbf{c} , that we want the camera to look at a target \mathbf{l} , and that a given up direction of the camera is \mathbf{u}' , as illustrated in Figure 4.5. We want to compute a basis consisting of three vectors, $\{\mathbf{r}, \mathbf{u}, \mathbf{v}\}$. We start by computing the view vector as $\mathbf{v} = (\mathbf{c} - \mathbf{l})/\|\mathbf{c} - \mathbf{l}\|$, i.e., the normalized vector from the target to the camera position. A vector looking to the “right” can then be computed as $\mathbf{r} = -(\mathbf{v} \times \mathbf{u}')/\|\mathbf{v} \times \mathbf{u}'\|$. The \mathbf{u}' vector is often not guaranteed to be pointing precisely up, so the final up vector is another cross product, $\mathbf{u} = \mathbf{v} \times \mathbf{r}$, which is guaranteed to be normalized since both \mathbf{v} and \mathbf{r} are normalized and perpendicular by construction. In the camera transform matrix, \mathbf{M} , that we will construct, the idea is to first translate everything so the camera position is at the origin, $(0, 0, 0)$, and then change the basis so that \mathbf{r} is aligned with $(1, 0, 0)$, \mathbf{u} with $(0, 1, 0)$, and \mathbf{v} with $(0, 0, 1)$. This is done by

$$\mathbf{M} = \underbrace{\begin{pmatrix} r_x & r_y & r_z & 0 \\ u_x & u_y & u_z & 0 \\ v_x & v_y & v_z & 0 \\ 0 & 0 & 0 & 1 \end{pmatrix}}_{\text{change of basis}} \underbrace{\begin{pmatrix} 1 & 0 & 0 & -t_x \\ 0 & 1 & 0 & -t_y \\ 0 & 0 & 1 & -t_z \\ 0 & 0 & 0 & 1 \end{pmatrix}}_{\text{translation}} = \begin{pmatrix} r_x & r_y & r_z & -\mathbf{t} \cdot \mathbf{r} \\ u_x & u_y & u_z & -\mathbf{t} \cdot \mathbf{u} \\ v_x & v_y & v_z & -\mathbf{t} \cdot \mathbf{v} \\ 0 & 0 & 0 & 1 \end{pmatrix}. \quad (4.20)$$

Note that when concatenating the translation matrix with the change of basis matrix, the translation $-\mathbf{t}$ is to the right since it should be applied first. One way to remember where to put the components of \mathbf{r} , \mathbf{u} , and \mathbf{v} is the following. We want \mathbf{r} to become $(1, 0, 0)$, so when multiplying a change of basis matrix with $(1, 0, 0)$, we can see that the first row in the matrix must be the elements of \mathbf{r} , since $\mathbf{r} \cdot \mathbf{r} = 1$. Furthermore, the second row and the third row must consist of vectors that are perpendicular to \mathbf{r} , i.e., $\mathbf{r} \cdot \mathbf{x} = 0$. When applying the same thinking also to \mathbf{u} and \mathbf{v} , we arrive at the change of basis matrix above. \square

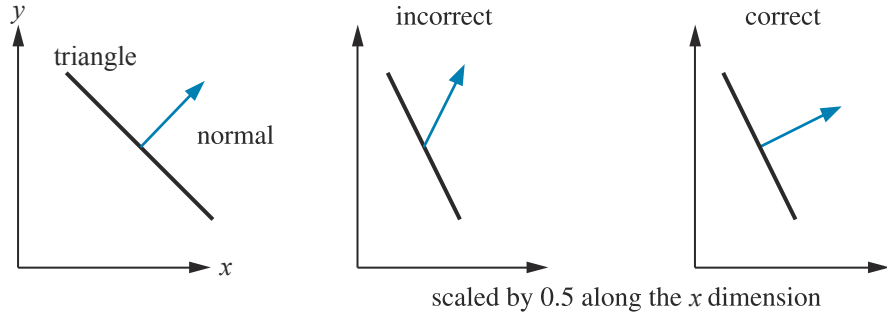


Figure 4.6. On the left is the original geometry, a triangle and its normal shown from the side. The middle illustration shows what happens if the model is scaled along the x -axis by 0.5 and the normal uses the same matrix. The right figure shows the proper transform of the normal.

4.1.7 Normal Transform

A single matrix can be used to consistently transform points, lines, triangles, and other geometry. The same matrix can also transform tangent vectors following along these lines or on the surfaces of triangles. However, this matrix cannot always be used to transform one important geometric property, the surface normal (and the vertex lighting normal). [Figure 4.6](#) shows what can happen if this same matrix is used.

Instead of multiplying by the matrix itself, the proper method is to use the transpose of the matrix's adjoint [227]. Computation of the adjoint is described in our online linear algebra appendix. The adjoint is always guaranteed to exist. The normal is not guaranteed to be of unit length after being transformed, so typically needs to be normalized.

The traditional answer for transforming the normal is that the transpose of the inverse is computed [1794]. This method normally works. The full inverse is not necessary, however, and occasionally cannot be created. The inverse is the adjoint divided by the original matrix's determinant. If this determinant is zero, the matrix is singular, and the inverse does not exist.

Even computing just the adjoint for a full 4×4 matrix can be expensive, and is usually not necessary. Since the normal is a vector, translation will not affect it. Furthermore, most modeling transforms are affine. They do not change the w -component of the homogeneous coordinate passed in, i.e., they do not perform projection. Under these (common) circumstances, all that is needed for normal transformation is to compute the adjoint of the upper left 3×3 components.

Often even this adjoint computation is not needed. Say we know the transform matrix is composed entirely of a concatenation of translations, rotations, and uniform scaling operations (no stretching or squashing). Translations do not affect the normal. The uniform scaling factors simply change the length of the normal. What is left is a series of rotations, which always yields a net rotation of some sort, nothing more.

The transpose of the inverse can be used to transform normals. A rotation matrix is defined by the fact that its transpose is its inverse. Substituting to get the normal transform, two transposes (or two inverses) give the original rotation matrix. Putting it all together, the original transform itself can also be used directly to transform normals under these circumstances.

Finally, fully renormalizing the normal produced is not always necessary. If only translations and rotations are concatenated together, the normal will not change length when transformed by the matrix, so no renormalizing is needed. If uniform scalings are also concatenated, the overall scale factor (if known, or extracted—[Section 4.2.3](#)) can be used to directly normalize the normals produced. For example, if we know that a series of scalings were applied that makes the object 5.2 times larger, then normals transformed directly by this matrix are renormalized by dividing them by 5.2. Alternately, to create a normal transform matrix that would produce normalized results, the original matrix’s 3×3 upper left could be divided by this scale factor once.

Note that normal transforms are not an issue in systems where, after transformation, the surface normal is derived from the triangle (e.g., using the cross product of the triangle’s edges). Tangent vectors are different than normals in nature, and are always directly transformed by the original matrix.

4.1.8 Computation of Inverses

Inverses are needed in many cases, for example, when changing back and forth between coordinate systems. Depending on the available information about a transform, one of the following three methods of computing the inverse of a matrix can be used:

- If the matrix is a single transform or a sequence of simple transforms with given parameters, then the matrix can be computed easily by “inverting the parameters” and the matrix order. For example, if $\mathbf{M} = \mathbf{T}(\mathbf{t})\mathbf{R}(\phi)$, then $\mathbf{M}^{-1} = \mathbf{R}(-\phi)\mathbf{T}(-\mathbf{t})$. This is simple and preserves the accuracy of the transform, which is important when rendering huge worlds [[1381](#)].
- If the matrix is known to be orthogonal, then $\mathbf{M}^{-1} = \mathbf{M}^T$, i.e., the transpose is the inverse. Any sequence of rotations is a rotation, and so is orthogonal.
- If nothing is known, then the adjoint method, Cramer’s rule, LU decomposition, or Gaussian elimination could be used to compute the inverse. Cramer’s rule and the adjoint method are generally preferable, as they have fewer branch operations; “if” tests are good to avoid on modern architectures. See [Section 4.1.7](#) on how to use the adjoint to invert transform normals.

The purpose of the inverse computation can also be taken into account when optimizing. For example, if the inverse is to be used for transforming vectors, then only the 3×3 upper left part of the matrix normally needs to be inverted (see the previous section).

4.2 Special Matrix Transforms and Operations

In this section, several matrix transforms and operations that are essential to real-time graphics will be introduced and derived. First, we present the Euler transform (along with its extraction of parameters), which is an intuitive way to describe orientations. Then we touch upon retrieving a set of basic transforms from a single matrix. Finally, a method is derived that rotates an entity around an arbitrary axis.

4.2.1 The Euler Transform

This transform is an intuitive way to construct a matrix to orient yourself (i.e., the camera) or any other entity in a certain direction. Its name comes from the great Swiss mathematician Leonhard Euler (1707–1783).

First, some kind of default view direction must be established. Most often it lies along the negative z -axis with the head oriented along the y -axis, as depicted in [Figure 4.7](#). The Euler transform is the multiplication of three matrices, namely the rotations shown in the figure. More formally, the transform, denoted \mathbf{E} , is given by [Equation 4.21](#):

$$\mathbf{E}(h, p, r) = \mathbf{R}_z(r)\mathbf{R}_x(p)\mathbf{R}_y(h). \quad (4.21)$$

The order of the matrices can be chosen in 24 different ways [\[1636\]](#); we present this one because it is commonly used. Since \mathbf{E} is a concatenation of rotations, it is also clearly orthogonal. Therefore its inverse can be expressed as $\mathbf{E}^{-1} = \mathbf{E}^T = (\mathbf{R}_z\mathbf{R}_x\mathbf{R}_y)^T = \mathbf{R}_y^T\mathbf{R}_x^T\mathbf{R}_z^T$, although it is, of course, easier to use the transpose of \mathbf{E} directly.

The Euler angles h , p , and r represent in which order and how much the head, pitch, and roll should rotate around their respective axes. Sometimes the angles are all called “rolls,” e.g., our “head” is the “ y -roll” and our “pitch” is the “ x -roll.” Also, “head” is sometimes known as “yaw,” such as in flight simulation.

This transform is intuitive and therefore easy to discuss in layperson’s language. For example, changing the head angle makes the viewer shake their head “no,” changing the pitch makes them nod, and rolling makes them tilt their head sideways. Rather than talking about rotations around the x -, y -, and z -axes, we talk about altering the head, pitch, and roll. Note that this transform can orient not only the camera, but also any object or entity as well. These transforms can be performed using the global axes of the world space or relative to a local frame of reference.

It is important to note that some presentations of Euler angles give the z -axis as the initial up direction. This difference is purely a notational change, though a potentially confusing one. In computer graphics there is a division in how the world is regarded and thus how content is formed: y -up or z -up. Most manufacturing processes, including 3D printing, consider the z -direction to be up in world space; aviation and sea vehicles consider $-z$ to be up. Architecture and GIS normally use z -up, as a building plan or map is two-dimensional, x and y . Media-related modeling systems often consider the y -direction as up in world coordinates, matching how we always describe a camera’s screen up direction in computer graphics. The difference between

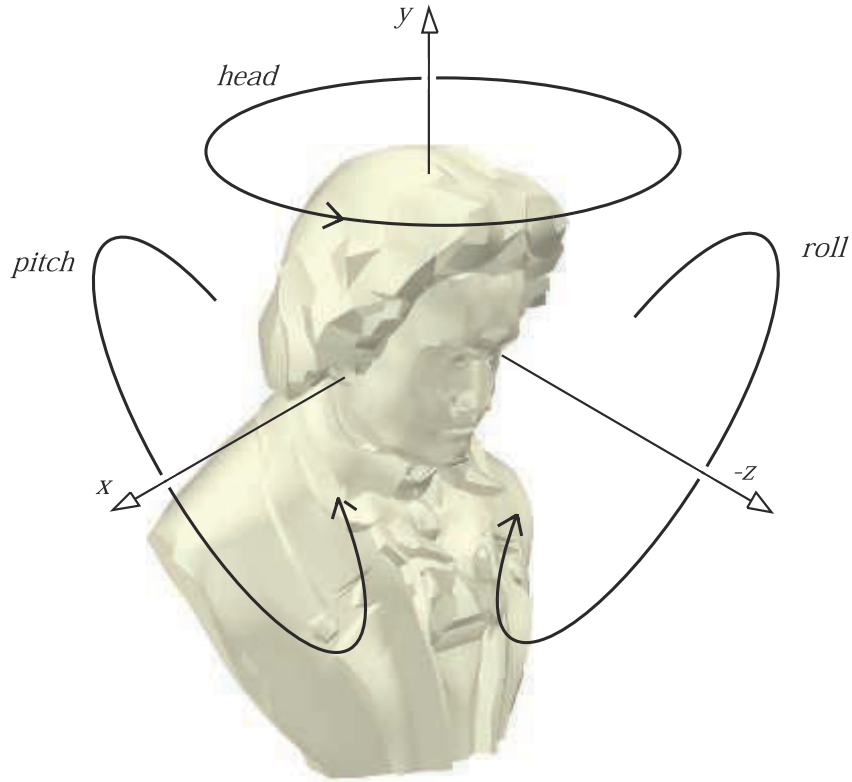


Figure 4.7. The Euler transform and how it relates to the way you change the *head*, *pitch*, and *roll* angles. The default view direction is shown, looking along the negative *-Z*-axis with the up direction along the *Y*-axis.

these two world up vector choices is just a 90° rotation (and possibly a reflection) away, but not knowing which is assumed can lead to problems. In this volume we use a world direction of *y*-up unless otherwise noted.

We also want to point out that the camera's up direction in its view space has nothing in particular to do with the world's up direction. Roll your head and the view is tilted, with its world-space up direction differing from the world's. As another example, say the world uses *y*-up and our camera looks straight down at the terrain below, a bird's eye view. This orientation means the camera has pitched 90° forward, so that its up direction in world space is $(0, 0, -1)$. In this orientation the camera has no *y*-component and instead considers $-z$ to be up in world space, but “*y* is up” remains true in view space, by definition.

While useful for small angle changes or viewer orientation, Euler angles have some other serious limitations. It is difficult to work with two sets of Euler angles in combi-

nation. For example, interpolation between one set and another is not a simple matter of interpolating each angle. In fact, two different sets of Euler angles can give the same orientation, so any interpolation should not rotate the object at all. These are some of the reasons that using alternate orientation representations such as quaternions, discussed later in this chapter, are worth pursuing. With Euler angles, you can also get something called gimbal lock, which will be explained next in [Section 4.2.2](#).

4.2.2 Extracting Parameters from the Euler Transform

In some situations, it is useful to have a procedure that extracts the Euler parameters, h , p , and r , from an orthogonal matrix. This procedure is shown in [Equation 4.22](#):

$$\mathbf{E}(h, p, r) = \begin{pmatrix} e_{00} & e_{01} & e_{02} \\ e_{10} & e_{11} & e_{12} \\ e_{20} & e_{21} & e_{22} \end{pmatrix} = \mathbf{R}_z(r)\mathbf{R}_x(p)\mathbf{R}_y(h). \quad (4.22)$$

Here we abandoned the 4×4 matrices for 3×3 matrices, since the latter provide all the necessary information for a rotation matrix. That is, the rest of the equivalent 4×4 matrix always contains zeros and a one in the lower right position.

Concatenating the three rotation matrices in [Equation 4.22](#) yields

$$\mathbf{E} = \begin{pmatrix} \cos r \cos h - \sin r \sin p \sin h & -\sin r \cos p & \cos r \sin h + \sin r \sin p \cos h \\ \sin r \cos h + \cos r \sin p \sin h & \cos r \cos p & \sin r \sin h - \cos r \sin p \cos h \\ -\cos p \sin h & \sin p & \cos p \cos h \end{pmatrix}. \quad (4.23)$$

From this it is apparent that the pitch parameter is given by $\sin p = e_{21}$. Also, dividing e_{01} by e_{11} , and similarly dividing e_{20} by e_{22} , gives rise to the following extraction equations for the head and roll parameters:

$$\frac{e_{01}}{e_{11}} = \frac{-\sin r}{\cos r} = -\tan r \quad \text{and} \quad \frac{e_{20}}{e_{22}} = \frac{-\sin h}{\cos h} = -\tan h. \quad (4.24)$$

Thus, the Euler parameters h (head), p (pitch), and r (roll) are extracted from a matrix \mathbf{E} using the function `atan2(y, x)` (see page 8 in [Chapter 1](#)) as in [Equation 4.25](#):

$$\begin{aligned} h &= \text{atan2}(-e_{20}, e_{22}), \\ p &= \arcsin(e_{21}), \\ r &= \text{atan2}(-e_{01}, e_{11}). \end{aligned} \quad (4.25)$$

However, there is a special case we need to handle. If $\cos p = 0$, we have gimbal lock ([Section 4.2.2](#)) and rotation angles r and h will rotate around the same axis (though possibly in different directions, depending on whether the p rotation angle was $-\pi/2$ or $\pi/2$), so only one angle needs to be derived. If we arbitrarily set $h = 0$ [[1769](#)], we get

$$\mathbf{E} = \begin{pmatrix} \cos r & \sin r \cos p & \sin r \sin p \\ \sin r & \cos r \cos p & -\cos r \sin p \\ 0 & \sin p & \cos p \end{pmatrix}. \quad (4.26)$$

Since p does not affect the values in the first column, when $\cos p = 0$ we can use $\sin r / \cos r = \tan r = e_{10}/e_{00}$, which gives $r = \text{atan2}(e_{10}, e_{00})$.

Note that from the definition of arcsin, $-\pi/2 \leq p \leq \pi/2$, which means that if \mathbf{E} was created with a value of p outside this interval, the original parameter cannot be extracted. That h , p , and r are not unique means that more than one set of the Euler parameters can be used to yield the same transform. More about Euler angle conversion can be found in Shoemake's 1994 article [1636]. The simple method outlined above can result in problems with numerical instability, which is avoidable at some cost in speed [1362].

When you use Euler transforms, something called *gimbal lock* may occur [499, 1633]. This happens when rotations are made so that one degree of freedom is lost. For example, say the order of transforms is $x/y/z$. Consider a rotation of $\pi/2$ around just the y -axis, the second rotation performed. Doing so rotates the local z -axis to be aligned with the original x -axis, so that the final rotation around z is redundant.

Mathematically, we have already seen gimbal lock in [Equation 4.26](#), where we assumed $\cos p = 0$, i.e., $p = \pm\pi/2 + 2\pi k$, where k is an integer. With such a value of p , we have lost one degree of freedom since the matrix only depends on one angle, $r + h$ or $r - h$ (but not both at the same time).

While Euler angles are commonly presented as being in $x/y/z$ order in modeling systems, a rotation around each local axis, other orderings are feasible. For example, $z/x/y$ is used in animation and $z/x/z$ in both animation and physics. All are valid ways of specifying three separate rotations. This last ordering, $z/x/z$, can be superior for some applications, as only when rotating π radians around x (a half-rotation) does gimbal lock occur. There is no perfect sequence that avoids gimbal lock. Euler angles nonetheless are commonly used, as animators prefer curve editors to specify how angles change over time [499].

EXAMPLE: CONSTRAINING A TRANSFORM. Imagine you are holding a (virtual) wrench that is gripping a bolt. To get the bolt into place, you have to rotate the wrench around the x -axis. Now assume that your input device (mouse, VR gloves, space-ball, etc.) gives you a rotation matrix, i.e., a rotation, for the movement of the wrench. The problem is that it is likely to be wrong to apply this transform to the wrench, which should rotate around only the x -axis. To restrict the input transform, called \mathbf{P} , to be a rotation around the x -axis, simply extract the Euler angles, h , p , and r , using the method described in this section, and then create a new matrix $\mathbf{R}_x(p)$. This is then the sought-after transform that will rotate the wrench around the x -axis (if \mathbf{P} now contains such a movement). \square

4.2.3 Matrix Decomposition

Up to this point we have been working under the assumption that we know the origin and history of the transformation matrix we are using. This is often not the case.

For example, nothing more than a concatenated matrix may be associated with some transformed object. The task of retrieving various transforms from a concatenated matrix is called *matrix decomposition*.

There are many reasons to retrieve a set of transformations. Uses include:

- Extracting just the scaling factors for an object.
- Finding transforms needed by a particular system. (For example, some systems may not allow the use of an arbitrary 4×4 matrix.)
- Determining whether a model has undergone only rigid-body transforms.
- Interpolating between keyframes in an animation where only the matrix for the object is available.
- Removing shears from a rotation matrix.

We have already presented two decompositions, those of deriving the translation and rotation matrix for a rigid-body transformation (Section 4.1.6) and deriving the Euler angles from an orthogonal matrix (Section 4.2.2).

As we have seen, it is trivial to retrieve the translation matrix, as we simply need the elements in the last column of the 4×4 matrix. We can also determine if a reflection has occurred by checking whether the determinant of the matrix is negative. To separate out the rotation, scaling, and shears takes more determined effort.

Fortunately, there are several articles on this topic, as well as code available online. Thomas [1769] and Goldman [552, 553] each present somewhat different methods for various classes of transformations. Shoemake [1635] improves upon their techniques for affine matrices, as his algorithm is independent of frame of reference and attempts to decompose the matrix to obtain rigid-body transforms.

4.2.4 Rotation about an Arbitrary Axis

Sometimes it is convenient to have a procedure that rotates an entity by some angle around an arbitrary axis. Assume that the rotation axis, \mathbf{r} , is normalized and that a transform should be created that rotates α radians around \mathbf{r} .

To do this, we first transform to a space where the axis around which we want to rotate is the x -axis. This is done with a rotation matrix, called \mathbf{M} . Then the actual rotation is performed, and we transform back using \mathbf{M}^{-1} [314]. This procedure is illustrated in Figure 4.8.

To compute \mathbf{M} , we need to find two axes that are orthonormal both to \mathbf{r} and to each other. We concentrate on finding the second axis, \mathbf{s} , knowing that the third axis, \mathbf{t} , will be the cross product of the first and the second axis, $\mathbf{t} = \mathbf{r} \times \mathbf{s}$. A numerically stable way to do this is to find the smallest component (in absolute value) of \mathbf{r} , and set it to 0. Swap the two remaining components, and then negate the first of them

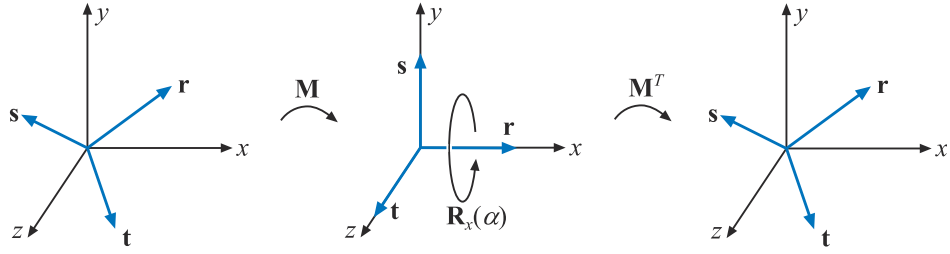


Figure 4.8. Rotation about an arbitrary axis, \mathbf{r} , is accomplished by finding an orthonormal basis formed by \mathbf{r} , \mathbf{s} , and \mathbf{t} . We then align this basis with the standard basis so that \mathbf{r} is aligned with the x -axis. The rotation around the x -axis is performed there, and finally we transform back.

(in fact, either of the nonzero components could be negated). Mathematically, this is expressed as [784]:

$$\begin{aligned}\bar{\mathbf{s}} &= \begin{cases} (0, -r_z, r_y), & \text{if } |r_x| \leq |r_y| \text{ and } |r_x| \leq |r_z|, \\ (-r_z, 0, r_x), & \text{if } |r_y| \leq |r_x| \text{ and } |r_y| \leq |r_z|, \\ (-r_y, r_x, 0), & \text{if } |r_z| \leq |r_x| \text{ and } |r_z| \leq |r_y|, \end{cases} \\ \mathbf{s} &= \bar{\mathbf{s}} / \| \bar{\mathbf{s}} \|, \\ \mathbf{t} &= \mathbf{r} \times \mathbf{s}.\end{aligned}\quad (4.27)$$

This guarantees that $\bar{\mathbf{s}}$ is orthogonal (perpendicular) to \mathbf{r} , and that $(\mathbf{r}, \mathbf{s}, \mathbf{t})$ is an orthonormal basis. Frisvad [496] presents a method without any branches in the code, which is faster but has lower accuracy. Max [1147] and Duff et al. [388] improve the accuracy of Frisvad's method. Whichever technique is employed, these three vectors are used to create a rotation matrix:

$$\mathbf{M} = \begin{pmatrix} \mathbf{r}^T \\ \mathbf{s}^T \\ \mathbf{t}^T \end{pmatrix}. \quad (4.28)$$

This matrix transforms the vector \mathbf{r} into the x -axis, \mathbf{s} into the y -axis, and \mathbf{t} into the z -axis. So, the final transform for rotating α radians around the normalized vector \mathbf{r} is then

$$\mathbf{X} = \mathbf{M}^T \mathbf{R}_x(\alpha) \mathbf{M}. \quad (4.29)$$

In words, this means that first we transform so that \mathbf{r} is the x -axis (using \mathbf{M}), then we rotate α radians around this x -axis (using $\mathbf{R}_x(\alpha)$), and then we transform back using the inverse of \mathbf{M} , which in this case is \mathbf{M}^T because \mathbf{M} is orthogonal.

Another method for rotating around an arbitrary, normalized axis \mathbf{r} by ϕ radians has been presented by Goldman [550]. Here, we simply present his transform:

$$\begin{aligned}\mathbf{R} &= \\ &\begin{pmatrix} \cos \phi + (1 - \cos \phi)r_x^2 & (1 - \cos \phi)r_xr_y - r_z \sin \phi & (1 - \cos \phi)r_xr_z + r_y \sin \phi \\ (1 - \cos \phi)r_xr_y + r_z \sin \phi & \cos \phi + (1 - \cos \phi)r_y^2 & (1 - \cos \phi)r_yr_z - r_x \sin \phi \\ (1 - \cos \phi)r_xr_z - r_y \sin \phi & (1 - \cos \phi)r_yr_z + r_x \sin \phi & \cos \phi + (1 - \cos \phi)r_z^2 \end{pmatrix}.\end{aligned}\quad (4.30)$$

In Section 4.3.2, we present yet another method for solving this problem, using quaternions. Also in that section are more efficient algorithms for related problems, such as rotation from one vector to another.

4.3 Quaternions

Although quaternions were invented back in 1843 by Sir William Rowan Hamilton as an extension to the complex numbers, it was not until 1985 that Shoemake [1633] introduced them to the field of computer graphics.¹ Quaternions are used to represent rotations and orientations. They are superior to both Euler angles and matrices in several ways. Any three-dimensional orientation can be expressed as a single rotation around a particular axis. Given this axis & angle representation, translating to or from a quaternion is straightforward, while Euler angle conversion in either direction is challenging. Quaternions can be used for stable and constant interpolation of orientations, something that cannot be done well with Euler angles.

A complex number has a real and an imaginary part. Each is represented by two real numbers, the second real number being multiplied by $\sqrt{-1}$. Similarly, quaternions have four parts. The first three values are closely related to axis of rotation, with the angle of rotation affecting all four parts (more about this in Section 4.3.2). Each quaternion is represented by four real numbers, each associated with a different part. Since quaternions have four components, we choose to represent them as vectors, but to differentiate them, we put a hat on them: $\hat{\mathbf{q}}$. We begin with some mathematical background on quaternions, which is then used to construct a variety of useful transforms.

4.3.1 Mathematical Background

We start with the definition of a quaternion.

Definition. A quaternion $\hat{\mathbf{q}}$ can be defined in the following ways, all equivalent.

$$\begin{aligned}\hat{\mathbf{q}} &= (\mathbf{q}_v, q_w) = iq_x + jq_y + kq_z + q_w = \mathbf{q}_v + q_w, \\ \mathbf{q}_v &= iq_x + jq_y + kq_z = (q_x, q_y, q_z), \\ i^2 &= j^2 = k^2 = -1, \quad jk = -kj = i, \quad ki = -ik = j, \quad ij = -ji = k.\end{aligned}\tag{4.31}$$

The variable q_w is called the real part of a quaternion, $\hat{\mathbf{q}}$. The imaginary part is \mathbf{q}_v , and i , j , and k are called imaginary units. \square

For the imaginary part, \mathbf{q}_v , we can use all the normal vector operations, such as addition, scaling, dot product, cross product, and more. Using the definition of the quaternion, the multiplication operation between two quaternions, $\hat{\mathbf{q}}$ and $\hat{\mathbf{r}}$, is derived

¹In fairness, Robinson [1502] used quaternions in 1958 for rigid-body simulations.

as shown below. Note that the multiplication of the imaginary units is noncommutative.

$$\begin{aligned}
 \text{Multiplication: } \hat{\mathbf{q}}\hat{\mathbf{r}} &= (iq_x + jq_y + kq_z + q_w)(ir_x + jr_y + kr_z + r_w) \\
 &= i(q_y r_z - q_z r_y + r_w q_x + q_w r_x) \\
 &\quad + j(q_z r_x - q_x r_z + r_w q_y + q_w r_y) \\
 &\quad + k(q_x r_y - q_y r_x + r_w q_z + q_w r_z) \\
 &\quad + q_w r_w - q_x r_x - q_y r_y - q_z r_z \\
 &= (\mathbf{q}_v \times \mathbf{r}_v + r_w \mathbf{q}_v + q_w \mathbf{r}_v, q_w r_w - \mathbf{q}_v \cdot \mathbf{r}_v).
 \end{aligned} \tag{4.32}$$

As can be seen in this equation, we use both the cross product and the dot product to compute the multiplication of two quaternions.

Along with the definition of the quaternion, the definitions of addition, conjugate, norm, and an identity are needed:

$$\text{Addition: } \hat{\mathbf{q}} + \hat{\mathbf{r}} = (\mathbf{q}_v, q_w) + (\mathbf{r}_v, r_w) = (\mathbf{q}_v + \mathbf{r}_v, q_w + r_w).$$

$$\text{Conjugate: } \hat{\mathbf{q}}^* = (\mathbf{q}_v, q_w)^* = (-\mathbf{q}_v, q_w).$$

$$\begin{aligned}
 \text{Norm: } n(\hat{\mathbf{q}}) &= \sqrt{\hat{\mathbf{q}}\hat{\mathbf{q}}^*} = \sqrt{\hat{\mathbf{q}}^*\hat{\mathbf{q}}} = \sqrt{\mathbf{q}_v \cdot \mathbf{q}_v + q_w^2} \\
 &= \sqrt{q_x^2 + q_y^2 + q_z^2 + q_w^2}.
 \end{aligned} \tag{4.33}$$

$$\text{Identity: } \hat{\mathbf{i}} = (\mathbf{0}, 1).$$

When $n(\hat{\mathbf{q}}) = \sqrt{\hat{\mathbf{q}}\hat{\mathbf{q}}^*}$ is simplified (result shown above), the imaginary parts cancel out and only a real part remains. The norm is sometimes denoted $\|\hat{\mathbf{q}}\| = n(\hat{\mathbf{q}})$ [1105]. A consequence of the above is that a multiplicative inverse, denoted by $\hat{\mathbf{q}}^{-1}$, can be derived. The equation $\hat{\mathbf{q}}^{-1}\hat{\mathbf{q}} = \hat{\mathbf{q}}\hat{\mathbf{q}}^{-1} = 1$ must hold for the inverse (as is common for a multiplicative inverse). We derive a formula from the definition of the norm:

$$n(\hat{\mathbf{q}})^2 = \hat{\mathbf{q}}\hat{\mathbf{q}}^* \iff \frac{\hat{\mathbf{q}}\hat{\mathbf{q}}^*}{n(\hat{\mathbf{q}})^2} = 1. \tag{4.34}$$

This gives the multiplicative inverse as shown below:

$$\text{Inverse: } \hat{\mathbf{q}}^{-1} = \frac{1}{n(\hat{\mathbf{q}})^2} \hat{\mathbf{q}}^*. \tag{4.35}$$

The formula for the inverse uses scalar multiplication, which is an operation derived from the multiplication seen in [Equation 4.3.1](#): $s\hat{\mathbf{q}} = (\mathbf{0}, s)(\mathbf{q}_v, q_w) = (s\mathbf{q}_v, sq_w)$, and $\hat{\mathbf{q}}s = (\mathbf{q}_v, q_w)(\mathbf{0}, s) = (s\mathbf{q}_v, sq_w)$, which means that scalar multiplication is commutative: $s\hat{\mathbf{q}} = \hat{\mathbf{q}}s = (s\mathbf{q}_v, sq_w)$.

The following collection of rules are simple to derive from the definitions:

Conjugate rules:

$$\begin{aligned} (\hat{\mathbf{q}}^*)^* &= \hat{\mathbf{q}}, \\ (\hat{\mathbf{q}} + \hat{\mathbf{r}})^* &= \hat{\mathbf{q}}^* + \hat{\mathbf{r}}^*, \\ (\hat{\mathbf{q}}\hat{\mathbf{r}})^* &= \hat{\mathbf{r}}^*\hat{\mathbf{q}}^*. \end{aligned} \quad (4.36)$$

Norm rules:

$$\begin{aligned} n(\hat{\mathbf{q}}^*) &= n(\hat{\mathbf{q}}), \\ n(\hat{\mathbf{q}}\hat{\mathbf{r}}) &= n(\hat{\mathbf{q}})n(\hat{\mathbf{r}}). \end{aligned} \quad (4.37)$$

Laws of Multiplication:

$$\begin{aligned} \text{Linearity:} \quad \hat{\mathbf{p}}(s\hat{\mathbf{q}} + t\hat{\mathbf{r}}) &= s\hat{\mathbf{p}}\hat{\mathbf{q}} + t\hat{\mathbf{p}}\hat{\mathbf{r}}, \\ &\quad (s\hat{\mathbf{p}} + t\hat{\mathbf{q}})\hat{\mathbf{r}} = s\hat{\mathbf{p}}\hat{\mathbf{r}} + t\hat{\mathbf{q}}\hat{\mathbf{r}}. \end{aligned} \quad (4.38)$$

Associativity: $\hat{\mathbf{p}}(\hat{\mathbf{q}}\hat{\mathbf{r}}) = (\hat{\mathbf{p}}\hat{\mathbf{q}})\hat{\mathbf{r}}$.

A unit quaternion, $\hat{\mathbf{q}} = (\mathbf{q}_v, q_w)$, is such that $n(\hat{\mathbf{q}}) = 1$. From this it follows that $\hat{\mathbf{q}}$ may be written as

$$\hat{\mathbf{q}} = (\sin \phi \mathbf{u}_q, \cos \phi) = \sin \phi \mathbf{u}_q + \cos \phi, \quad (4.39)$$

for some three-dimensional vector \mathbf{u}_q , such that $\|\mathbf{u}_q\| = 1$, because

$$\begin{aligned} n(\hat{\mathbf{q}}) &= n(\sin \phi \mathbf{u}_q, \cos \phi) = \sqrt{\sin^2 \phi (\mathbf{u}_q \cdot \mathbf{u}_q) + \cos^2 \phi} \\ &= \sqrt{\sin^2 \phi + \cos^2 \phi} = 1 \end{aligned} \quad (4.40)$$

if and only if $\mathbf{u}_q \cdot \mathbf{u}_q = 1 = \|\mathbf{u}_q\|^2$. As will be seen in the next section, unit quaternions are perfectly suited for creating rotations and orientations in a most efficient way. But before that, some extra operations will be introduced for unit quaternions.

For complex numbers, a two-dimensional unit vector can be written as $\cos \phi + i \sin \phi = e^{i\phi}$. The equivalent for quaternions is

$$\hat{\mathbf{q}} = \sin \phi \mathbf{u}_q + \cos \phi = e^{\phi \mathbf{u}_q}. \quad (4.41)$$

The log and the power functions for unit quaternions follow from [Equation 4.41](#):

Logarithm: $\log(\hat{\mathbf{q}}) = \log(e^{\phi \mathbf{u}_q}) = \phi \mathbf{u}_q,$

$$(4.42)$$

Power: $\hat{\mathbf{q}}^t = (\sin \phi \mathbf{u}_q + \cos \phi)^t = e^{\phi t \mathbf{u}_q} = \sin(\phi t) \mathbf{u}_q + \cos(\phi t).$

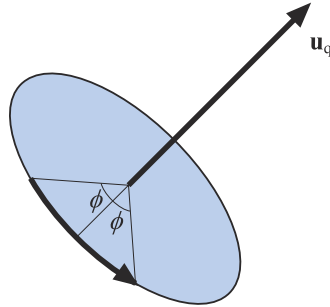


Figure 4.9. Illustration of the rotation transform represented by a unit quaternion, $\hat{\mathbf{q}} = (\sin \phi \mathbf{u}_q, \cos \phi)$. The transform rotates 2ϕ radians around the axis \mathbf{u}_q .

4.3.2 Quaternion Transforms

We will now study a subclass of the quaternion set, namely those of unit length, called *unit quaternions*. The most important fact about unit quaternions is that they can represent any three-dimensional rotation, and that this representation is extremely compact and simple.

Now we will describe what makes unit quaternions so useful for rotations and orientations. First, put the four coordinates of a point or vector $\mathbf{p} = (p_x \ p_y \ p_z \ p_w)^T$ into the components of a quaternion $\hat{\mathbf{p}}$, and assume that we have a unit quaternion $\hat{\mathbf{q}} = (\sin \phi \mathbf{u}_q, \cos \phi)$. One can prove that

$$\hat{\mathbf{q}} \hat{\mathbf{p}} \hat{\mathbf{q}}^{-1} \quad (4.43)$$

rotates $\hat{\mathbf{p}}$ (and thus the point \mathbf{p}) around the axis \mathbf{u}_q by an angle 2ϕ . Note that since $\hat{\mathbf{q}}$ is a unit quaternion, $\hat{\mathbf{q}}^{-1} = \hat{\mathbf{q}}^*$. See [Figure 4.9](#).

Any nonzero real multiple of $\hat{\mathbf{q}}$ also represents the same transform, which means that $\hat{\mathbf{q}}$ and $-\hat{\mathbf{q}}$ represent the same rotation. That is, negating the axis, \mathbf{u}_q , and the real part, q_w , creates a quaternion that rotates exactly as the original quaternion does. It also means that the extraction of a quaternion from a matrix can return either $\hat{\mathbf{q}}$ or $-\hat{\mathbf{q}}$.

Given two unit quaternions, $\hat{\mathbf{q}}$ and $\hat{\mathbf{r}}$, the concatenation of first applying $\hat{\mathbf{q}}$ and then $\hat{\mathbf{r}}$ to a quaternion, $\hat{\mathbf{p}}$ (which can be interpreted as a point \mathbf{p}), is given by [Equation 4.44](#):

$$\hat{\mathbf{r}}(\hat{\mathbf{q}} \hat{\mathbf{p}} \hat{\mathbf{q}}^*) \hat{\mathbf{r}}^* = (\hat{\mathbf{r}} \hat{\mathbf{q}}) \hat{\mathbf{p}} (\hat{\mathbf{r}} \hat{\mathbf{q}})^* = \hat{\mathbf{c}} \hat{\mathbf{p}} \hat{\mathbf{c}}^*. \quad (4.44)$$

Here, $\hat{\mathbf{c}} = \hat{\mathbf{r}} \hat{\mathbf{q}}$ is the unit quaternion representing the concatenation of the unit quaternions $\hat{\mathbf{q}}$ and $\hat{\mathbf{r}}$.

Matrix Conversion

Since one often needs to combine several different transforms, and most of them are in matrix form, a method is needed to convert [Equation 4.43](#) into a matrix. A quaternion,